Phase Transitions and Spatio-Temporal Fluctuations in Stochastic Lattice Lotka–Volterra Models

Mauro Mobilia,[1, 2, *] Ivan T. Georgiev,[3, 2, †] and Uwe C. Täuber[2, ‡]

[1]*Arnold Sommerfeld Center for Theoretical Physics and Center for NanoScience,*
Department of Physics, Ludwig-Maximilians-Universität München, D-80333 Munich, Germany
[2]*Department of Physics and Center for Stochastic Processes in Science and Engineering,*
Virginia Polytechnic Institute and State University, Blacksburg, Virginia 24061-0435, U.S.A.
[3]*Integrated Finance Limited, 630 Fifth Avenue, Suite 450, New York, NY 10111, U.S.A.*
(Dated: February 9, 2008)

We study the general properties of stochastic two-species models for predator-prey competition and coexistence with Lotka–Volterra type interactions defined on a d-dimensional lattice. Introducing spatial degrees of freedom and allowing for stochastic fluctuations generically invalidates the classical, deterministic mean-field picture. Already within mean-field theory, however, spatial constraints, modeling locally limited resources, lead to the emergence of a continuous active-to-absorbing state phase transition. Field-theoretic arguments, supported by Monte Carlo simulation results, indicate that this transition, which represents an extinction threshold for the predator population, is governed by the directed percolation universality class. In the active state, where predators and prey coexist, the classical center singularities with associated population cycles are replaced by either nodes or foci. In the vicinity of the stable nodes, the system is characterized by essentially stationary localized clusters of predators in a sea of prey. Near the stable foci, however, the stochastic lattice Lotka–Volterra system displays complex, correlated spatio-temporal patterns of competing activity fronts. Correspondingly, the population densities in our numerical simulations turn out to oscillate irregularly in time, with amplitudes that tend to zero in the thermodynamic limit. Yet in finite systems these oscillatory fluctuations are quite persistent, and their features are determined by the intrinsic interaction rates rather than the initial conditions. We emphasize the robustness of this scenario with respect to various model perturbations.

I. INTRODUCTION

Since Lotka and Volterra's seminal and pioneering works [1, 2], many decades ago, modeling of interacting, competing species has received considerable attention in the fields of biology, ecology, mathematics [3, 4, 5, 6, 7, 8, 9, 10, 11, 12, 13, 14, 15], and, more recently, in the physics literature as well [16, 17, 18, 19, 20, 21, 22, 23, 24, 25, 26, 27]. In their remarkably simple deterministic model, Lotka and Volterra considered two coupled nonlinear differential equations that mimic the temporal evolution of a two-species system of competing predator and prey populations. They demonstrated that coexistence of both species was not only possible but inevitable in their model. Moreover, similar to observations in real populations, both predator and prey densities in this deterministic system display regular oscillations in time, with both the amplitude and the period determined by the prescribed initial conditions (only near the center fixed point associated with the coexistence of the two populations is the oscillation frequency solely given in terms of the intrinsic interaction rates, see Sec. II.A below). However, despite the undisputed mathematical elegance of these results, and its consequent ubiquity in textbooks [3, 4, 5, 6, 7], the original Lotka–Volterra model (LVM) is often severely criticized on the grounds of being biologically too simplistic and therefore unrealistic [5], and mathematically unstable with respect to model modifications [7].

In this paper, we aim at drawing a comprehensive, detailed picture of the *stochastic* dynamics, defined on a d-dimensional lattice, of two competing populations with Lotka–Volterra type predation interaction. The systems under consideration are 'individual-based' lattice models, where each lattice site can be occupied by a given (finite) number of particles. We shall formulate the *stochastic lattice Lotka–Volterra model* (SLLVM) in the natural language of a reaction–diffusion lattice gas model, i.e., in terms of appropriate stochastic particle hopping and creation and annihilation processes defined on a lattice, and will here investigate them by means of various methods of the theory of nonequilibrium statistical mechanics, including mean-field approximations, Monte Carlo computer simulations, field-theoretic representations and renormalization group arguments. With these techniques, we are thus able to consider and discuss the role of spatial constraints, spatio-temporal fluctuations and correlations, and finite-size effects. We shall argue that although the criticisms against the classical LVM definitely pertain to the original deterministic rate equations, introducing spatial degrees of freedom and allowing for stochasticity [13] actually renders the corre-

*Electronic address: mauro.mobilia@physik.lmu.de
†Electronic address: igeorgiev@ifltd.com
‡Electronic address: tauber@vt.edu

sponding two-species reaction system considerably richer, definitely more interesting, and perhaps even more realistic. In addition, in stark contrast with the deterministic LVM, the SLLVM scenario turns out to be remarkably robust with respect to model modifications, and thus appears to provide a quite generic picture of two-species predator-prey interactions.

In recent years, population dynamics has received considerable attention from the statistical physics community. In particular, a variety of so-called 'individual-based', or stochastic, lattice predator-prey models have been investigated, e.g., in Refs. [16, 17, 18, 19, 20, 21, 22, 23], employing largely mean-field-type approaches (including refined versions, such as the pair approximation of Refs. [16, 22]) and Monte Carlo simulations, mostly in two dimensions. Among the main issues addressed by these papers are the phase diagrams of these stochastic lattice Lotka–Volterra systems (see, e.g., Refs. [16, 17, 18, 22, 25, 26, 27]), the critical properties near the predator extinction threshold, typically argued to be governed by the scaling exponents of the directed percolation (DP) universality class [16, 17, 18, 25, 26], and the presence or absence of (stochastic) oscillations, whose amplitudes were reported in Refs. [17, 18, 21] to (globally) decrease as the system size was increased.

Since it would be impossible (and well beyond our scope here) to provide a complete survey of the numerous contributions of statistical physicists to the fascinating field of population dynamics, we choose, for the sake of clarity, to briefly discuss more specifically some work on lattice predator–prey models that we have found to be particularly relevant for the issues considered in this article. In Refs. [17, 18], the authors considered various two-species four-state models (in the absence of diffusion, each lattice site is either empty, occupied by a single predator or prey, or by both a predator and prey) and noticed that both extinction and coexistence of the two populations are possible. They found that there exists a sharp continuous transition between the predator extinction phase and the active predator–prey coexistence phase. Numerical studies of the (static) critical properties near the predator extinction threshold (mainly in one and two dimensions) revealed that its critical exponents are consistent with those of DP [28, 29] (see below). In addition, in Refs. [17, 18] the oscillatory behavior displayed by the densities of the coexisting populations in some region of the active parameter space was studied as well. It was reported that in one and two dimensions the population densities showed characteristic erratic oscillations whose amplitude vanishes in the thermodynamic limit (even in the presence of long-range interactions), while it was argued that the oscillation amplitude may remain *finite* in three dimensions [17]. The authors of Ref. [21] considered a non-diffusive three-state model (each site can be empty, or occupied either by a predator or a prey) interacting according to a *cyclic* scheme. This system can in fact be mapped onto the so-called 'rock-scissors-paper' (or three-state cyclic

Lotka–Volterra) model [11, 23], well-known in the field of game theory [11]. The (mean-field) rate equations associated with that model actually admit a constant of motion [11, 21] which in turn implies cycles in the phase portrait, describing regular oscillations of the densities of predators and prey. However, numerical simulations of the stochastic version of that model on two-dimensional lattices led to a completely different behavior: The system was shown to display erratic oscillations whose amplitude vanished on a global scale for large lattices, but which were reported to persist on a smaller scale. These were explained in Ref. [21] as being associated with 'small oscillators' (actually fluctuations) that are out of phase. Also, the fractal dimension of the patterns developed on the square lattice as result of the spatial fluctuations of the reactants was investigated [21]. We also would like to mention that Boccara et al. [25] studied a two-dimensional automaton network predator-prey model (a three-state system) with parallel updating for all the reactions except for 'smart motion' (updated sequentially) of the predators (prey) which propagate toward the direction of highest (lowest) prey (predator) density. The authors of Ref. [25] studied the phase portrait, finding a stable coexistence state which may exhibit noisy cyclic behavior associated with complex patterns, and computing critical exponents, which in some regime are in reasonable agreement with the DP values. Later, other authors [26] considered the two-dimensional lattice-gas (with sequential updating) version of the model introduced by Boccara et al. and studied numerically its phase diagram and critical properties, finding again results consistent with the DP universality class. In addition, for the two-dimensional model of Refs. [26], Rozenfeld and Albano argued that, in good agreement with mean-field results, there exists a region of the phase diagram where the densities of species "exhibit self-sustained oscillations", with amplitudes that remain finite in the thermodynamic limit. As such a result was somewhat surprising, but could stem from the long-range interaction between predators and prey displayed in the model of Refs. [26], Lipowski, willing also to test the general validity of the scenario outlined in Refs. [26], checked that the range of interaction did *not* affect the characteristics of the oscillatory behavior displayed in two dimensions by the model of Ref. [17]: Actually, the amplitude of the oscillations was always found to vanish in the thermodynamic limit.

Before specifying further on two-species (stochastic) predator–prey models, for the sake of completeness we give a brief overview of some properties of the *multi-species* Lotka–Volterra rate equations. In general, for n particle or population species the latter read (with $i = 1, \ldots, n$) [3, 9, 11]:

$$\frac{dx_i(t)}{dt} = x_i(t)\left(r_i + \sum_{j=1}^{n} \alpha_{i,j}\, x_j(t)\right), \qquad (1)$$

where x_i denotes the species i, the r_i are the intrinsic growth ($r_i > 0$) or decay ($r_i < 0$) rates, and $\alpha_{i,j}$ represents the *interaction* matrix that encodes the competition

'reaction' between species i and j. For general $\alpha_{i,j}$ and an arbitrary number $n > 2$ of species, many questions remain wide open. One of the most intriguing (and less understood) features is the fact that the deterministic equations (1) may generate *chaotic* behavior already for only three species ($n = 3$) [3, 11]. In the case where $\alpha_{i,j} = -\alpha_{j,i}$, and thus $\alpha_{i,i} = 0$ (which means that there is no nonlinear interaction within the same species), it has been shown that Eq. (1) allows for a constant of motion (conserved first integral) [9]. Nonetheless, also in this situation, for an even number of species with $n \geq 4$ it was demonstrated that Eq. (1) can display chaotic behavior resembling Hamiltonian chaos [10]. We also mention that when three or more species are in *cyclic* competition according to a dynamics described by Eqs. (1), i.e., the rate equations are invariant under cyclic permutations of the species, quite intriguing behavior may emerge: For some time it looks as if one species were bound to become the unique 'survivor'; then its density drops and it is replaced with another apparently dominant species, and after some time a third species seems to become dominant, and so on cyclically, involving all n species [11, 12].

In the case of a food chain with n components, where there is interaction (competition) among agents of the same species and where the first species serves as the prey for the second, which is the prey of the third and so on, the only nonzero entries of the interaction matrix of Eq. (1) are $\alpha_{i,i} < 0$, $\alpha_{i,i+1} < 0$, $\alpha_{i,i-1} > 0$ ($\alpha_{1,0} = 0$), and also $r_1 > 0$, $r_i < 0$ for $i > 1$. In this case, it is known [11] that the situation with $n = 2$ is generic and already captures the features of the multi-species system. In Sec. II.C we shall discuss in detail the properties of a system [Eqs. (6,7)] which can be recast into the above two-species case. Little is known as yet about spatial multi-species Lotka–Volterra systems defined on lattices, where spatial fluctuations generally invalidate (at least in low dimensions) the predictions from the mean-field rate equations (1). We note, however, that adding multiplicative noise as appropriate for the existence of inactive, absorbing states transforms Eqs. (1) to the Langevin equations for multi-species directed percolation processes, whose critical properties were shown by Janssen to be generically described by the DP universality class [30]. A remarkable exception is the stochastic cyclic Lotka–Volterra model [23], mimicking a simple cyclic food chain of length n, where the species A_i ($i = 1, \dots, n$) react according to the scheme $A_1 + A_2 \rightarrow 2A_1$, $A_2 + A_3 \rightarrow 2A_2, \dots, A_{n-1} + A_n \rightarrow 2A_{n-1}$, $A_n + A_1 \rightarrow 2A_n$. For this system, Frachebourg and Krapivsky [23] showed analytically (within a so-called Kirkwood decoupling scheme), and confirmed numerically, that in any dimension there is a critical number of species n_c above which the system reaches a frozen steady state, i.e., there is *fixation* [23], characterized by inert, non-fluctuating domains at whose interfaces all dynamics ceases (for example, in one dimension, $A_1 \dots A_1 A_3 \dots A_3 A_5 \dots A_5 A_2 \dots A_2 A_4 \dots A_4$). In one dimension, the minimal number of species in order to have fixation is five; for $n < 5$ the systems coarsens:

a large domain of a single species eventually spans the whole lattice. In two and three dimensions it was found that $n_c = 14$ and $n_c = 23$, respectively; for $n < n_c$, the steady state is reactive in $d = 2, 3$.

All the above models are non-diffusive in the sense that there is no explicit mechanism allowing the mixing of the system: the agents are considered as *immobile* (but species may still spread because of the particle production processes, since new offspring have to be put to adjacent sites). Clearly, as noted by other authors [17, 21, 25, 26, 27], a more realistic description of the predator–prey interaction should include the possibility for the agents to move. In fact, in ecosystems a prey tend to avoid the interaction with an incoming predator, while the predators aim to pursue the prey. In the absence of mixing processes, one can expect that the stochastic lattice predator–prey model should display features like fixation (which is interesting but does not seem realistic from an ecological perspective). One approach, followed here, is to allow the system to be mixed via particle (predators and prey) *diffusion*. Another approach, considered elsewhere for a model with next-nearest-neighbor interaction [31], is to consider a nearest-neighbor exchange process (among any agents: predators, prey and empty sites) referred to as 'stirring'. Interestingly, completely different results are obtained for systems mixed through diffusion or stirring, respectively: While in Sec. III.C we shall explain that diffusion does not affect the critical and other generic properties of the system under consideration here, the exchange process is in fact capable of completely washing out the subtle correlations induced by long-range interactions. We discuss this latter issue in detail elsewhere [31].

After this general discussion, let us anticipate the main results of this present work (of which a partial and brief account has recently been outlined in Ref. [31]):

- We provide a comparison of various mean-field predictions with the results of numerical Monte Carlo simulations in dimensions $1 \leq d \leq 4$, addressing the phase diagram, the structure of the phase portrait, the existence and properties of the predator extinction phase transition, and other issues (Secs. II.C and III.C).

- We analytically derive some exact properties of the SLLVM (Sec. III.B), quantitatively study the phase portrait and characterize the properties of the intriguing spatial structures in the oscillatory regime of the active coexistence state by numerically computing several correlation functions (Sec. III.C).

- We study the emergence of transient stochastic oscillations in the SLLVM and discuss the functional dependence of their characteristic frequency as well as the dependence of their amplitude on the system size (Sec. III.C).

- We provide a renormalization group argument, based on a field theory representation of the corre-

sponding master equation, that establishes that the active to absorbing extinction transition is indeed governed by the directed percolation (DP) universality class (Sec. III.D).

Our results thus both confirm and supplement earlier work, where, as discussed above, some of these issues have already been considered for related, but significantly different, systems such as the four-state models of Refs. [17, 18], or the cyclic three-state model of Ref. [21]. In particular, we shall show that the mean-field rate equations [Eqs. (6,7)] for the model under consideration here already provide a *qualitatively* (albeit *not* quantitatively) correct description of the behavior of the corresponding stochastic lattice system, of which they therefore capture the essential features (in dimensions $d > 1$).

The organization of this article is the following: Section II is devoted to a review of the properties of the deterministic two-species LVM. Section II.A covers the basic properties of the original Lotka–Volterra coupled rate equations (see Ref. [7], Vol. I, Chap. 3). The fundamental features of the corresponding zero-dimensional stochastic model are reviewed in Sec. II.B [4, 19]. In Secs. II.C and II.D, we consider the LVM rate equations subject to finite carrying capacities, and its spatial extension with diffusive particle propagation [20] (see also Ref. [7], Vol. II, Chap.1). Section III is devoted to the two-species stochastic lattice Lotka–Volterra model (SLLVM), as introduced in Sec. III.A. Some exact properties of the SLLVM are discussed in Sec. III.B. Section III.C is devoted to the results from our Monte Carlo simulations of the SLLVM: Dynamical features in the active phase as well as the critical properties near the predator extinction threshold are presented and discussed in detail here. In Sec. III.D, we present a field-theoretic analysis of the critical properties of the SLLVM. Section IV is devoted to our conclusions.

II. PRELIMINARIES: GENERIC PROPERTIES OF THE LOTKA–VOLTERRA MODEL (LVM) AND MEAN-FIELD THEORY

A. The two-species Lotka–Volterra rate equations

Following Lotka and Volterra's original work [1, 2], we consider two chemical or biological species, the 'predators' A and 'prey' B, in competition: the predators consume the prey and *simultaneously* reproduce with rate $\lambda > 0$. In addition, the prey may reproduce with rate σ and the predators are assumed to spontaneously die with rate μ. Neglecting any spatial variations of the concentrations, which we shall denote by $a(\boldsymbol{x}, t)$ and $b(\boldsymbol{x}, t)$ for species A and B, respectively, the heuristic mean-field rate equations for this reaction model are given by the classical coupled nonlinear Lotka–Volterra (LV) differen-

tial equations [1, 2]:

$$\dot{a}(t) = \lambda\, a(t)\, b(t) - \mu\, a(t) \;, \qquad (2)$$

$$\dot{b}(t) = \sigma\, b(t) - \lambda\, a(t)\, b(t) \;, \qquad (3)$$

where the dot denotes the time derivative. Note that within this mean-field approximation, we may view the parameters $-\mu = \sigma_A - \mu_A$ and $\sigma = \sigma_B - \mu_B$ as the net population growth rates for competing birth/death processes ($A \to A + A$ and $A \to \oslash$, where $\oslash$ denotes an empty 'spot') with rates σ_A and μ_A, respectively, and similarly for species B. For $\mu > 0$ and $\sigma < 0$, clearly both populations will die out exponentially, whereas $\mu < 0$ and $\sigma > 0$ leads to unbounded population growth. Therefore, interesting feedback interactions between the 'prey' B and the 'predators' A, which would become extinct in the absence of the prey, occur only if both μ and σ (as well as λ) are positive.

The coupled deterministic evolution equations (2), (3) have as stationary states (fixed points) $(a^*, b^*) = (0, 0)$ (extinction), $(0, \infty)$ (predators extinct, Malthusian prey proliferation), and $(a_c, b_c) = (\sigma/\lambda, \mu/\lambda)$ (species coexistence). For positive μ and σ, the 'trivial' steady states with $a = 0$ and $b = 0$ and ∞ are both linearly unstable [in the absence of predation, $\lambda = 0$, $(0, \infty)$ is stable].

Notice, however, that they both constitute *absorbing* stationary states, since neither can be left through the involved reactions alone. Linearizing about the nontrivial coexistence stationary state, $\delta a(t) = a(t) - a_c$, $\delta b(t) = b(t) - b_c$, one obtains to first order in δA and δB: $\delta\dot{a}(t) = \sigma\, \delta b(t)$, and $\delta\dot{b}(t) = -\mu\, \delta a(t)$. The eigenvalues of the corresponding Jacobian (also occasionally termed stability or community matrix) are $\pm i\sqrt{\mu\sigma}$, which suggests purely oscillatory kinetics in the vicinity of the neutrally stable fixed point (center singularity) (a_c, b_c). Indeed, one finds the general periodic solutions $\delta a(t) = \delta a(0)\, \cos\left(\sqrt{\mu\sigma}\, t\right) + \delta b(0)\, \sqrt{\sigma/\mu}\, \sin\left(\sqrt{\mu\sigma}\, t\right)$, and $\delta b(t) = -\delta a(0)\, \sqrt{\mu/\sigma}\, \sin\left(\sqrt{\mu\sigma}\, t\right) + \delta b(0)\, \cos\left(\sqrt{\mu\sigma}\, t\right)$, with characteristic frequency $\omega = \sqrt{\mu\sigma}$.

Going beyond linear stability analysis, one easily confirms that the quantity

$$K(t) = \lambda[a(t) + b(t)] - \sigma \ln a(t) - \mu \ln b(t) \qquad (4)$$

represents a conserved first integral for any phase space trajectory, $\dot{K}(t) = 0$. Quite generally, therefore, Eqs. (2), (3) yield periodic oscillations of both species concentrations, whose amplitudes (and in the nonlinear regime, also whose frequencies) are determined by the *initial* conditions $a(0)$ and $b(0)$, and according to Eq. (4) neither $a(t)$ nor $b(t)$ can ever vanish. The emergence of purely oscillatory kinetics in this classical Lotka–Volterra model, irrespective of the involved reaction rates, and in character only determined by the initial conditions, is clearly not a realistic feature [5, 7].

B. The zero-dimensional stochastic Lotka–Volterra model

Instead of the regular cycles, completely determined by the *initial* conditions, predicted by the rate equations (2), (3), one would more realistically typically expect stable stationary states with fixed concentrations, and/or the possibility of extinction thresholds. Indeed, the conservation law for $K(t)$ and the related property that the eigenvalues of the linearized kinetics near coexistence are purely imaginary, constitute very special features of the *deterministic* model equations — there is in fact no underlying physical background for the conserved quantity (4). Correspondingly, the above center singularity is *unstable* with respect to perturbations: namely, either with respect to introducing modifications of the model equations, spatial degrees of freedom, and/or stochasticity. For obviously, when the number of predators becomes very low, a chance fluctuation may lead the system into the absorbing state with $a = 0$. Consider the zero-dimensional stochastic Lotka–Volterra model that is governed by the following master equation, stating the gain and loss balance for the temporal evolution of the probability of finding A predators and B prey in the system,

$$
\begin{aligned}
\dot{P}(A,B;t) &= \lambda(A-1)(B+1)P(A-1,B+1;t) \\
&+ \mu(A+1)P(A+1,B;t) + \sigma(B-1)P(A,B-1;t) \\
&- (\mu A + \sigma B + \lambda A B)P(A,B;t) \,.
\end{aligned} \tag{5}
$$

In this description, the system has *discrete* degrees of freedom, and it can be verified that its only stable stationary state ($\dot{P} = 0$) is $P_s(A=0, B=0) = 1$ and $P_s(A \neq 0, B \neq 0) = 0$ [4]. Therefore, *asymptotically* as $t \to \infty$ the empty state will be reached, which is *absorbing*, since all processes cease there, and no fluctuation can drive the system out of it anymore. However, at *finite* times such stochastic Lotka–Volterra systems still display quite intriguing dynamics: namely, inevitable fluctuations tend to push the system away from the trivial steady state and induce erratic population oscillations that almost resemble the deterministic cycles. This 'resonant amplification mechanism' is always present in finite populations and can significantly delay extinction [19]. We shall later, in Sec. III.C, discuss the analog of this mechanism in the spatially extended models.

C. Mean-field rate equations with finite carrying capacities

In the ecological and biological literature, at the rate equation level, population models such as (2), (3) are rendered more 'realistic' by introducing *growth-limiting* terms that describe a finite 'carrying capacity' [5, 7]. In a similar manner, in a spatial system one may need to take into account that the *local* population densities cannot exceed some given, bound value, which typically depends on external factors; this amounts to introducing

spatial constraints, e.g., in a lattice model, restrictions on the maximum possible occupation number on each site. There are various possibilities to introduce carrying capacities; here we consider the very natural choice of limiting the effective reproduction term in Eq.(3) for the prey, in the form $\sigma b(t)\left[1 - \zeta^{-1} a(t) - \rho^{-1} b(t)\right]$, where $0 \leq \zeta^{-1} \leq \rho^{-1} \leq 1$. In the absence of the predators, ρ represents the prey carrying capacity. In the presence of predators, it is further diminished by the cross-species interactions. In the lattice model, these choices reflect the fact that prey reproduce only when an 'empty spot' is available in its immediate vicinity. The resulting rate equations now read (with $0 < \rho \leq \zeta$):

$$
\begin{aligned}
\dot{a}(t) &= a(t)\left[\lambda b(t) - \mu\right], \tag{6} \\
\dot{b}(t) &= \sigma b(t)\left[1 - \zeta^{-1} a(t) - \rho^{-1} b(t)\right] - \lambda a(t) b(t) \,. \tag{7}
\end{aligned}
$$

As shown in Sec. III.B, when $\zeta = \rho = 1$, Eqs. (6) and (7) can be interpreted as the mean-field versions of the *exact microscopic* equations derived from a stochastic lattice formulation (based on the corresponding master equation) where each lattice site may at most be occupied by a single particle. Obviously, in this case $0 \leq a(t) + b(t) \leq 1$ (provided that this inequality holds initially at time $t = 0$). [Indeed, even when Eq. (7) cannot be related to some microscopic dynamics, it is readily verified that still $0 \leq \zeta^{-1} a(t) + \rho^{-1} b(t) \leq 1$, provided one starts with a 'physical' initial condition, i.e., $0 \leq \zeta^{-1} a(0) + \rho^{-1} b(0) \leq 1$ and, in addition, $0 < \rho \leq \zeta$ holds.]

The coupled rate equations (6) and (7) have three fixed points. The two obvious ones are $(a_1^*, b_1^*) = (0,0)$ (total population extinction) and $(a_2^*, b_2^*) = (0, \rho)$, corresponding to a system filled with prey up to its carrying capacity. The only nontrivial fixed point, associated with the coexistence of both populations, is (a_3^*, b_3^*), with

$$
a_3^* = \frac{\zeta\sigma}{\zeta\lambda + \sigma}\left(1 - \frac{\mu}{\lambda\rho}\right) \,, \quad b_3^* = \frac{\mu}{\lambda} \,. \tag{8}
$$

Species coexistence is obviously possible only when $\lambda > \mu/\rho$. For fixed predator death rate μ and prey carrying capacity ρ, the predator population dies out if $\lambda \leq \lambda_c = \mu/\rho$, which represents the predator *extinction threshold*. For $\lambda \to \lambda_c$ from above, the stationary predator density tends to zero continuously; hence predator extinction constitutes a continuous nonequilibrium phase transition from the active coexistence phase to an inactive, absorbing state: once all predators are gone, no mechanism, not even stochastic fluctuations, allows them to ever reappear in the system.

Before proceeding with the linear stability analysis of Eqs. (6) and (7), we remark that there exists a *Lyapunov function* $V(a,b)$ [7, 11] associated with those equations. In fact, with

$$
\begin{aligned}
V(a,b) &= \lambda\left[b_3^* \ln b(t) - b(t)\right] \\
&+ (\lambda + \sigma/\zeta)\left[a_3^* \ln a(t) - a(t)\right], \tag{9}
\end{aligned}
$$

we have $\dot{V}(a,b) = \frac{\lambda\sigma}{\rho}\left[b_3^* - b(t)\right]^2 \geq 0$ and $\dot{V}(a_3^*, b_3^*) = 0$. According to Lyapunov's theorem, every flow $(a(t), b(t))$ is contained in $\{(a,b)|\dot{V}(a,b) = 0\}$. Therefore, since $V(a,b) > 0 \quad \forall (a,b) \neq (a_3^*, b_3^*)$ and the neighborhood of (a_3^*, b_3^*) represents an invariant subset (the so-called ω-limit property in Chap. 2 of Ref. [11]), it follows that (a_3^*, b_3^*) is indeed *globally stable* (when physically accessible, i.e., for $\lambda > \mu/\rho$). Only when $\rho = \infty$, as is the case in the classical LV equations, $V(a,b) = 0$, and in this situation $(a_3^*, b_3^*) \to \left(\frac{\zeta\sigma}{\zeta\lambda+\sigma}, \frac{\mu}{\lambda}\right)$ is *not* globally stable.

There is general no methods to find a Lyapunov function (provided it even exists) associated with a given set of coupled ordinary differential equations. One thus often relies on generic mathematical results, such as Kolmogorov's theorem (see Refs. [3, 8] and references therein) and the so-called Bendixson–Dulac test (Refs. [11, 32]) to establish the existence of a stable fixed point or limit cycle. As explained in Appendix A, Kolmogorov's theorem does not apply to Eqs. (6), (7), while the Bendixson–Dulac test yields that these equations do *not* admit periodic orbits (as long as there is a finite carrying capacity, i.e. $\rho < \infty$).

We now proceed with an analysis of the properties of the various fixed points of the rate equations (6) and (7) by means of linear stability analysis [7]. To this end, we need to diagonalize the Jacobian matrix $(i = 1, 2, 3)$

$$J = \begin{pmatrix} \lambda b_i^* - \mu & \lambda a_i^* \\ -\left(\frac{\sigma}{\zeta} + \lambda\right)b_i^* & \sigma\left(1 - \frac{2b_i^*}{\rho}\right) - \left(\frac{\sigma}{\zeta} + \lambda\right)a_i^* \end{pmatrix}. \quad (10)$$

This gives the eigenvalues associated with the fixed point $(0,0)$ to be $\epsilon_+ = \sigma$ and $\epsilon_- = -\mu$, which implies that the empty lattice fixed point is a saddle point (unstable in the b direction), for any value of ζ and ρ. For the fixed point $(0, \rho)$ (system filled with prey), the eigenvalues read $\epsilon_+ = \rho\lambda - \mu$ and $\epsilon_- = -\sigma$. This means that $(0, \rho)$ is a *stable node* provided $\lambda < \lambda_c = \mu/\rho$. When $\lambda > \lambda_c$, where the nontrivial fixed point (8) yields a positive predator density, ϵ_+ becomes positive, and $(0, \rho)$ turns into a saddle point (unstable in the a direction). This result also confirms that in the absence of any local density restriction on the prey, i.e., in the limit $\rho \to \infty$, the fixed point $(0, \rho) \to (0, \infty)$ becomes unstable for any $\lambda > 0$.

For the nontrivial fixed point given by Eq. (8), the corresponding eigenvalues are

$$\epsilon_\pm = -\frac{\sigma\mu}{2\lambda\rho}\left[1 \pm \sqrt{1 - \frac{4\lambda\rho}{\sigma}\left(\frac{\lambda\rho}{\mu} - 1\right)}\right], \quad (11)$$

and the different emerging scenarios can be summarized as follows:

- for $\lambda \in]\lambda_c, \lambda_s]$ or $\sigma > \sigma_s$, where $\lambda_c = \mu/\rho$ and $\lambda_s = \frac{\mu}{2\rho}\left(1 + \sqrt{1 + \frac{\sigma}{\mu}}\right)$ and $\sigma_s = 4\lambda\rho\left(\frac{\lambda\rho}{\mu} - 1\right) > 0$, the eigenvalues are real with $\epsilon_\pm < 0$: the fixed point is a *stable node*;

- for $\lambda \in]\lambda_s, \infty[$ or $\sigma < \sigma_s$, the eigenvalues $\epsilon_\pm$ have both real and imaginary parts; in this case $\Re(\epsilon_\pm) < 0$ and $|\Im(\epsilon_\pm)| \neq 0$, provided that $\rho < \infty$ ($\mu\sigma/\rho\lambda > 0$): the nontrivial fixed point (8) is an *attractive focus*;

- if $\rho \to \infty$ and/or if $\mu\sigma/\rho\lambda \to 0$ (with finite μ and σ), the real part of the eigenvalues vanishes, whence $\epsilon_\pm \to \pm i\sqrt{\mu\sigma}$. In this extreme situation the nontrivial fixed point at $\rho = \infty$ becomes a center singularity, and we encounter periodic cycles in the phase portrait. In the case when ρ is finite and $\mu\sigma/\rho\lambda \to 0$, the fixed point evolves towards one of the phase space boundaries, and no cyclic behavior can be established.

It is worthwhile noticing that these scenarios quantitatively differ from those predicted by the rate equations in the models of Refs. [17, 21] and turn out to be essentially independent of the actual value of ζ, which is the parameter that controls the spatial restrictions of the predators on the prey population.

As a result of this discussion, on the rate equation level, it turns out that the growth-limiting constraints (as long as $\rho^{-1} > 0$) generically invalidate the classical Lotka–Volterra picture. Interestingly, the density restrictions induce a *continuous* active to absorbing phase transition, namely an extinction threshold for the predator population at $\lambda_c = \mu/\rho$, which can be accessed by varying the reaction rates. At mean-field level (then confirmed by numerical simulations of the related stochastic models), extinction phase transitions were also reported in Refs. [16, 18, 26]. In the vicinity of the phase transition at λ_c (with σ and μ held fixed), the density of predators approaches its stationary value linearly according to Eqs. (6), (7): $a_3^* \sim (\lambda - \lambda_c)^{\beta_{\mathrm{MF}}}$, with $\beta_{\mathrm{MF}} = 1$. Moreover, depending on these rates, the only stable fixed point, corresponding to the coexistence of both populations of predators and prey, is either a node or a focus, and therefore approached either directly or in an oscillatory manner. Near the predator extinction threshold, the active fixed point is a node; deeper in the population coexistence phase, it changes its character to a focus. In Sec. III.C, we shall test the validity of the results arising from the deterministic mean-field rate equations (6) and (7) by considering stochastic lattice predator–prey models defined on lattices and formulated in a microscopic setting (i.e., starting from stochastic dynamical rules) taking into account internal noise (fluctuations).

D. The deterministic reaction–diffusion equations (with finite carrying capacities)

To account for the spatial structure on a rate equation level, and guaranteeing asymptotic stability of the coexistence state with both nonvanishing predator and prey populations, one may introduce spatial degrees of freedom. This effectively allows the prey to 'escape' via

diffusion, which in turn requires the predators to 'pursue' them, thus effectively generating delay terms in the kinetics that stabilize the nontrivial steady state [7]. As previously, this can be done in a heuristic fashion with finite carrying capacity ρ and additional growth-limiting term ζ for the prey, and adding diffusive terms $\nabla^2 a(\boldsymbol{x}, t)$ and $\nabla^2 b(\boldsymbol{x}, t)$ to Eqs. (6) and (7), with diffusivities D_A and D_B:

$$\frac{\partial a(\boldsymbol{x}, t)}{\partial t} = D_A \nabla^2 a(\boldsymbol{x}, t) + \lambda \, a(\boldsymbol{x}, t) \, b(\boldsymbol{x}, t) - \mu \, a(\boldsymbol{x}, t) \ ,$$

$$\frac{\partial b(\boldsymbol{x}, t)}{\partial t} = D_B \nabla^2 b(\boldsymbol{x}, t) - \lambda \, a(\boldsymbol{x}, t) \, b(\boldsymbol{x}, t) \qquad (12)$$
$$+ \sigma \, b(\boldsymbol{x}, t) \left[1 - \zeta^{-1} a(\boldsymbol{x}, t) - \rho^{-1} b(\boldsymbol{x}, t) \right] \ .$$

For instance, it is straightforward to construct one-dimensional wavefront solutions to the deterministic coupled reaction–diffusion equations (12) of the form $a(x, t) = a(x + ct)$ and $b(x, t) = b(x + ct)$, which interpolate between the stationary states $(0, \rho)$ and (a_3^*, b_3^*). In fact, depending on the rate parameters, there exist two types of such travelling waves of 'pursuit and evasion', namely either with monotonic or oscillatory approach to the stable state [20]; these correspond to the different scenarios discussed in the previous Sec. II.C. For $D_B = 0$, one finds a minimum wavefront propagation velocity $c \geq [4 D_A (\lambda \rho - \mu)]^{1/2}$ (see Ref. [7], Vol. II, Chap. 1.2.).

As we shall explain in Sec. III.C (see Fig. 2), such 'pursuit and evasion' waves in the predator and prey density fields arise naturally in the SLLVM in a certain region of parameter space, even in the absence of explicit diffusion of either species. We also mention that the problem of velocity selection for reaction fronts starting from a microscopic description, e.g., from the associated master equation, for the underlying stochastic processes is a rather subtle issue [33, 34]. For some two-state models, a field-theoretic representation has been useful to derive a stochastic differential equation that properly represents the underlying stochastic process [34]. However, to the best of our knowledge no similar treatment has as yet been devised for Lotka–Volterra type interactions.

III. THE STOCHASTIC LATTICE LOTKA–VOLTERRA MODEL (SLLVM)

In the remainder of this paper, we study and carefully discuss the role of spatial structure and intrinsic stochastic noise on the physical properties of systems with Lotka–Volterra type predator–prey interaction, starting from a microscopic (stochastic) formulation. We shall compare the results of the SLLVM with those predicted by the rate equations (6), (7) and will show that there is qualitative agreement for many overall features (in dimensions $d > 1$), but there are also important differences. We shall investigate the site-restricted stochastic version of the lattice Lotka–Volterra model.

Starting from the master equation governing its stochastic kinetics, we shall employ numerical Monte Carlo simulations as well as field-theoretic arguments.

A. The SLLVM (with site restrictions) as a *stochastic* reaction–diffusion model

We define the SLLVM with site restrictions as a *microscopic* reaction–diffusion system on a periodic hypercubic lattice of linear size L, whose sites $\boldsymbol{j}$ are labeled by their components $\boldsymbol{j} = (j_1, \ldots, j_d)$, where d denotes the spatial dimension, and the unit vectors are represented by $\boldsymbol{e}_i$ for $i \in (1, \ldots, d)$. Each lattice site can either be empty ($\oslash$), occupied by a 'predator' (A particle) or by a 'prey' (B particle). Multiple occupancy is *not* allowed, and the stochastic rules determining the system's dynamics are defined as follows:

- $A \xrightarrow[\mu]{} \oslash$: death of a predator with rate μ;

- $A\oslash \xrightarrow[D/z]{} \oslash A$ and $B\oslash \xrightarrow[D/z]{} \oslash B$: nearest-neighbor hopping (diffusion) with rate D/z;

- $B\oslash \xrightarrow[\sigma/z]{} BB$: branching (offspring generation) of a prey with rate σ/z;

- $AB \xrightarrow[\lambda/z]{} AA$: predation interaction: a predator consumes a prey and produces an offspring with rate λ/z.

In the above rules the quantity $z = 2d$ represents the lattice coordination number; all processes occur isotropically in space, i.e., there is no spatial bias in the reaction rates. We also notice that the process with rate μ represents a single-site reaction, whereas the processes with rates D, σ, and λ describe nearest-neighbor two-site reactions.

Microscopically, each configuration $\mathcal{C} = \mathcal{C}_{\{A, B, \oslash\}}$ of the system at time t is characterized by a probabilistic weight $P(\mathcal{C}, t)$. The temporal evolution of this probability distribution is governed by a master equation:

$$\dot{P}(\mathcal{C}, t) = \sum_{\mathcal{C}' \neq \mathcal{C}} W(\mathcal{C}' \to \mathcal{C}) \, P(\mathcal{C}', t)$$
$$- \sum_{\mathcal{C}' \neq \mathcal{C}} W(\mathcal{C} \to \mathcal{C}') \, P(\mathcal{C}, t) \ , \qquad (13)$$

where the transition from the configuration $\mathcal{C}'$ to $\mathcal{C}$ (during an infinitesimal time interval dt) occurs through a single reaction event with nonzero rate $W(\mathcal{C}' \to \mathcal{C})$. The first term on the right-hand-side of Eq. (13) is the 'gain term' accounting for contributions entering the configuration $\mathcal{C}$, while the second ('loss') term captures the processes leaving $\mathcal{C}$. Of course, the configurations $\mathcal{C}$ and $\mathcal{C}'$, as well as the transition rates, should be compatible with the processes underlying the dynamics. For instance, in one dimension, the configuration

$\mathcal{C} = \{B, A, \oslash, B, A, \oslash, \ldots, A, \oslash, A, \oslash, B\}$ is compatible with $\mathcal{C}' = \{A, A, \oslash, B, A, \oslash, \ldots, A, \oslash, A, \oslash, B\}$, and in this case the transition $\mathcal{C} \to \mathcal{C}'$ occurs with a rate $W(\mathcal{C} \to \mathcal{C}') = \lambda/z$. Specifically, to account for the site restriction and the fact that we are dealing with a three-state model, the master equation can be rewritten in a matrix form by introducing suitable 3×3 operators, which are the direct generalization of Pauli's spin-1/2 operators (see, e.g., Ref. [35]). Within this spin-like reformulation, which is by now standard in the study of reaction–diffusion systems (see, e.g., Ref. [36, 37] for reviews), the master equation (13) can formally be rewritten as an 'imaginary-time Schrödinger' equation where the 'stochastic Hamiltonian' H, which is the Markovian generator, is in general not Hermitian. Taking advantage of such a reformulation, the equations of motion of all the observables, e.g., the density of particles, correlation functions, etc. can be obtained in a systematic algebraic fashion using the corresponding quantum physical Heisenberg picture (see, e.g., Ref. [36]). In this language, the equation of motion of the average value of an observable of interest, say $\mathcal{O}$ (density, correlator, ...), reads $\frac{d}{dt}\langle\mathcal{O}(t)\rangle = \sum_{\mathcal{C}} \mathcal{O}(t) P(\mathcal{C}, t) = \langle[H, \hat{\mathcal{O}}(t)]\rangle$, where the square bracket denotes the usual commutator and $\hat{\mathcal{O}}$ is the operator whose eigenvalue is $\mathcal{O}$.

In addition to allowing us to derive exact properties of the phase portrait of the SLLVM (see below), the stochastic Hamiltonian reformulation of the master equation is the most suitable approach on which to build a field-theoretic analysis of the critical properties of the system. Such a treatment is the scope of Section III.D below.

B. SLLVM equations of motion and some exact properties

Let us now formulate the stochastic equation of motion for the density of the A and B particles, denoted respectively as before $a(\boldsymbol{j}, t) = \langle n_{\boldsymbol{j}}^A(t)\rangle$ and $b(\boldsymbol{j}, t) = \langle n_{\boldsymbol{j}}^B(t)\rangle$. The stochastic variable $n_{\boldsymbol{j}}^A$ $(n_{\boldsymbol{j}}^B)$ represents the occupation number at site $\boldsymbol{j}$ by A (B) particles: $n_{\boldsymbol{j}}^A = 1$ $(n_{\boldsymbol{j}}^B = 1)$ if the site $\boldsymbol{j}$ is occupied by a predator (prey), and 0 otherwise. Obviously, it follows that $\langle n_{\boldsymbol{j}}^{\oslash}(t)\rangle = 1 - \langle n_{\boldsymbol{j}}^A(t)\rangle - \langle n_{\boldsymbol{j}}^B(t)\rangle$. Considering a translationally invariant system, it is then straightforward to obtain the following *exact* equations of motion for the concentrations of the predators and the prey from the master equation (13):

$$\dot{a}(t) = \lambda c_{AB}(t) - \mu a(t) , \tag{14}$$
$$\dot{b}(t) = \sigma [b(t) - c_{BB}(t) - c_{AB}(t)] - \lambda c_{AB}(t) , \tag{15}$$

where $c_{AA}(t) = \langle n_{\boldsymbol{j}}^A n_{\boldsymbol{j}+\boldsymbol{e_i}}^A\rangle(t)$, $c_{BB}(t) = \langle n_{\boldsymbol{j}}^B n_{\boldsymbol{j}+\boldsymbol{e_i}}^B\rangle(t)$, and $c_{AB}(t) = \langle n_{\boldsymbol{j}}^A n_{\boldsymbol{j}+\boldsymbol{e_i}}^B\rangle(t) = \langle n_{\boldsymbol{j}}^B n_{\boldsymbol{j}+\boldsymbol{e_i}}^A\rangle(t)$ represent the two-point correlation functions. Notice that the diffusion rate D and the coordination number z do not appear explicitly in Eqs. (14) and (15). However, they would en-

ter the equations of motion for the two-site probability distributions, i.e., the correlators $c_{AB}(t)$ and $c_{BB}(t)$.

It is clear from these equations of motion that the quantity K in Eq. (4) is no longer a first integral of the motion of the stochastic model (with the site restrictions, this is even true on the mean-field level, as we saw in Sec. II.C). Even though it is not possible to solve Eqs. (14) and (15) in a closed form, owing to the emerging infinite hierarchy of higher-order correlations, we can still obtain some useful and nontrivial information on the phase portrait. Let us denote by a^* and b^* the stationary concentrations of the predators and the prey, respectively, and by c_{BB}^* and c_{AB}^* the stationary values of the correlators from Eqs. (14) and (15). As the site occupation number restrictions imply $0 \le a(t), b(t), c_{BB}(t), c_{AB}(t) \le 1$, we thus have $0 \le \mu a^* = \lambda c_{AB}^*$ and $0 \le b^* - \frac{\sigma+\lambda}{\sigma\lambda}\mu a^* = c_{BB}^* \le 1$. Thus, as a direct consequence of our reformulation of the problem, we arrive at the following inequalities, which considerably restrict the physically available phase portrait:

$$0 \le a^* \le \min\left(\frac{\lambda}{\mu}, 1\right); \quad 0 \le b(t) \le 1 ,$$
$$0 \le a(t) + b(t) \le 1 ,$$
$$0 \le b^* - \frac{\sigma+\lambda}{\sigma\lambda}\mu a^* \le 1 . \tag{16}$$

We emphasize that the inequalities (16) are *exact* and obtained from very general considerations starting from the master equation. In this sense they intrinsically account for the *spatial* and *stochastic* nature of the underlying reaction–diffusion system. Upon ignoring any spatial fluctuations and correlations, which amounts to assuming the factorizations $c_{AB}(t) = a(t) b(t)$ and $c_{BB}(t) = b(t)^2$, after substitution into Eqs. (14) and (15) one recovers the deterministic mean-field rate equations (6) and (7) with $\rho = \zeta = 1$. This implies that the site restrictions on a mean-field level correspond to a finite prey carrying capacity.

C. Monte Carlo simulations of the SLLVM

In this section, we report our results from direct Monte Carlo simulations in one, two, and three dimensions for the lattice reaction–diffusion (or stochastic lattice gas) SLLVM introduced in Sec. III.A.

The SLLVM under consideration is simulated on a simple cubic lattice with periodic boundary conditions. Each lattice site can be in one of the three possible states: occupied by a prey, by a predator, or empty. The algorithm that we use for simulating our model is the following:

- randomly choose a site on the lattice and generate a random number (RN) uniformly distributed between zero and one to perform the four possible reactions of our SLLVM (with rates D, μ, λ and σ), namely either of the four following processes:
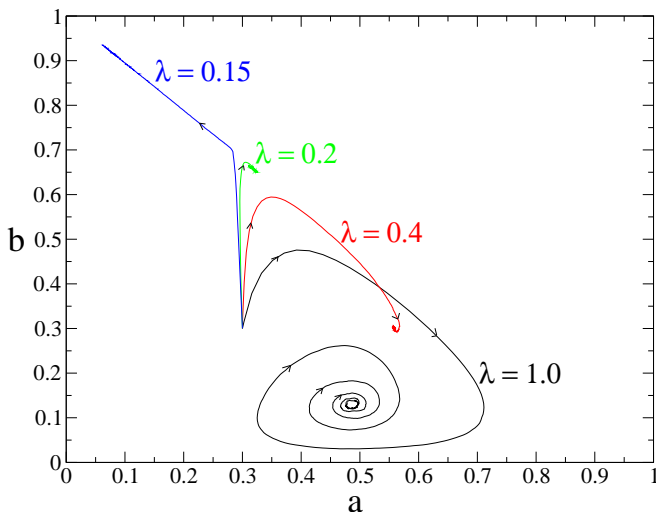
FIG. 1: (Color online.) Typical trajectories above in the predator/prey coexistence phase depicting the phase portrait for the NN model on a (512×512) lattice. All runs start from random initial configuration with $a(0) = b(0) = 0.3$ and fixed rates $D = 0$, $\sigma = 4.0$, $\mu = 0.1$, and $\lambda = 0.15, 0.20, 0.40, 1.0$, respectively. For high values of λ we observe the typical spirals (the fixed point is a focus) in phase space, while for small values of λ (typically $\lambda < 0.4$) the fixed point is a node.

- if $RN < 1/4$ then randomly select one of the neighboring sites, and with rate D exchange the contents of the two sites if the neighboring site is empty;

- if $1/4 \leq RN < 1/2$ and if the site holds a predator, then with rate μ the site will become empty;

- if $1/2 \leq RN < 3/4$ and if the site holds a predator, choose a neighboring site at random; if that site holds a prey then with rate λ the neighboring site becomes a predator;

- if $3/4 \leq RN < 1$ and if the site holds a prey, randomly select a neighboring site; if that site is empty, then with a rate of σ the neighboring site becomes a prey.

One Monte Carlo step (MCS) is completed when the above steps are repeated as many times as there are number of the sites on the lattice. We have numerically checked that explicit diffusion does not usually alter the behavior of the system, even when diffusion is fast compared to the reactions: we have run simulations with D up to 1000 times bigger than all the other rates, and not observed any qualitative changes. Specifically, we have verified that the spatial structures such as those depicted in Figs. 2 and 3 were also obtained for small (or zero), intermediate, and large ($D = 0 \ldots 1000$) diffusivities. Similarly, the critical properties of the system (scaling exponents), as discussed in detail hereafter, were found to be independent of the values of the diffusion rate (at least in the range $D = 0 \ldots 1000$). Hence, without loss of generality and for the sake of simplicity, in many simulations we have set $D = 0$. Note that in this case, the particle

offspring production processes effectively generate diffusive proliferation of the two species.

Typical trajectories in the active phase (in 2D), all starting from random initial configurations, are depicted in Fig. 1. In qualitative agreement with the mean-field analysis, the fixed point can either be a node, which in its vicinity is reached via straight trajectories, or, for larger values of the predation rate λ, a focus that is approached in spiralling paths. Of course, the agreement with the mean-field theory is *not* fully quantitative: in fact, there are fluctuations not accounted for in the rate equations (6), (7). However, the qualitative agreement (in dimensions $d > 1$) reported here on the structure of the phase portrait as predicted by the mean-field equations and as obtained for the SLLVM is remarkable, and actually was not observed in other stochastic predator–prey systems [17, 21]. For the various rates and the related values of the fixed points a^* and b^*, we can also check that the inequalities (16) are actually obeyed.

The three pictures on Fig. 2 show three consecutive snapshots of the system in the predator–prey coexistence phase on a two-dimensional lattice for parameter values for which the fixed point is a focus. We observe the formation of highly nontrivial patterns that display strong correlations between the predator and prey populations [38]. These typical snapshots illustrate how starting from a spatially homogeneous random initial configuration this simple model may develop amazingly rich patterns in the steady state where one can clearly distinguish fluctuating localized spots of predator and prey activity. In this regime we see that in the early stages of the system's temporal evolution rings of prey are formed that are followed by predators in the inner part of the rings (the leftmost picture in Fig. 2). These rings subsequently grow with time and merge upon encounter. The steady state is maintained by a dynamical equilibrium of moving fronts of prey (with a typical length set by the value of the stochastic parameters) followed by predators that in turn leave behind empty sites that are needed for the next wave of prey to step in.

To gain further quantitative insight on the complex spatial structure (see Fig. 2) and on the fluctuations characterizing the system, we have computed numerically the static (and translationally invariant) correlation functions between various species, defined as $C_{\alpha,\beta}(x) = \langle n_{j+x}^{\alpha} n_j^{\beta} \rangle(\infty) - \langle n_{j+x}^{\alpha}(\infty) \rangle \langle n_j^{\beta}(\infty) \rangle$, where $\alpha, \beta \in (A, B, \oslash)$. For the sake of illustration, in Figs. 4, 5, and 6 we report all the six connected correlation functions of the system, namely $C_{A,B}(x)$, $C_{\oslash,\oslash}(x)$, $C_{A,A}(x)$, $C_{B,B}(x)$, $C_{A,\oslash}$, and $C_{B,\oslash}$ measured for various two-dimensional situations. The static correlation functions were obtained on 256×256 lattices where the data were taken every 200 MCS for a run of total 2×10^9 MCS. When the rates σ, D, and μ are held fixed, the behaviors displayed by $C_{A,B}(x)$, $C_{\oslash,\oslash}(x)$, $C_{A,A}(x)$, $C_{B,B}(x)$, $C_{A,\oslash}$, and $C_{B,\oslash}$ can be qualitatively understood taking into account the fact that the predation reaction $AB \to AA$ occurs more likely when λ is raised (as a consequence, the
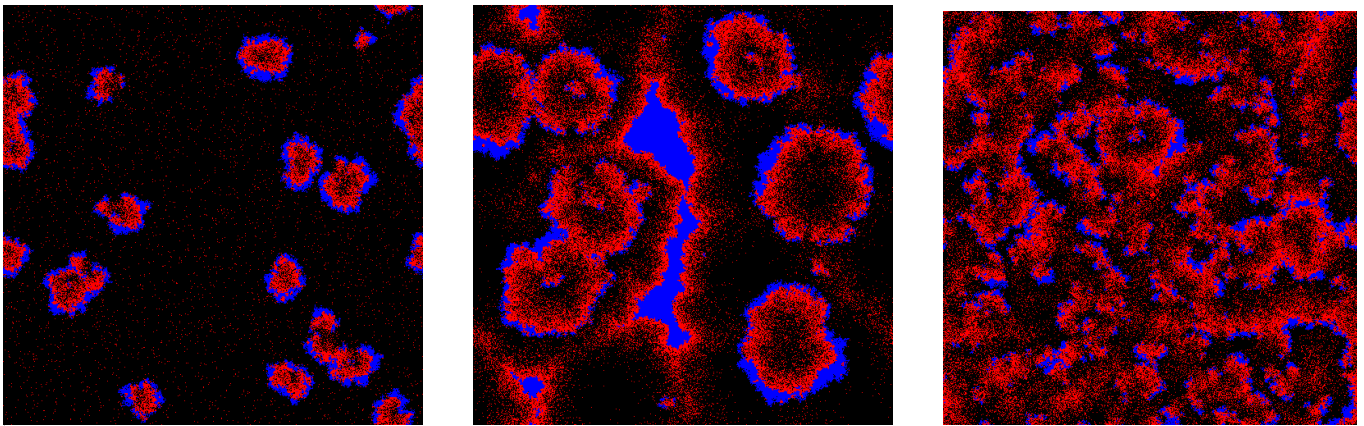
FIG. 2: (Color online.) Snapshots of the time evolution (time increases from left to right) of the two-dimensional SLLVM model in the species coexistence phase, when the fixed point is a focus. The red, blue, and dark dots respectively represent the prey, predators, and empty lattice sites. The rates here are $D = 0$, $\sigma = 4.0$, $\mu = 0.1$, and $\lambda = 2.2$. The system is initially homogeneous with densities $a(0) = b(0) = 1/3$ and the lattice size is 512×512.
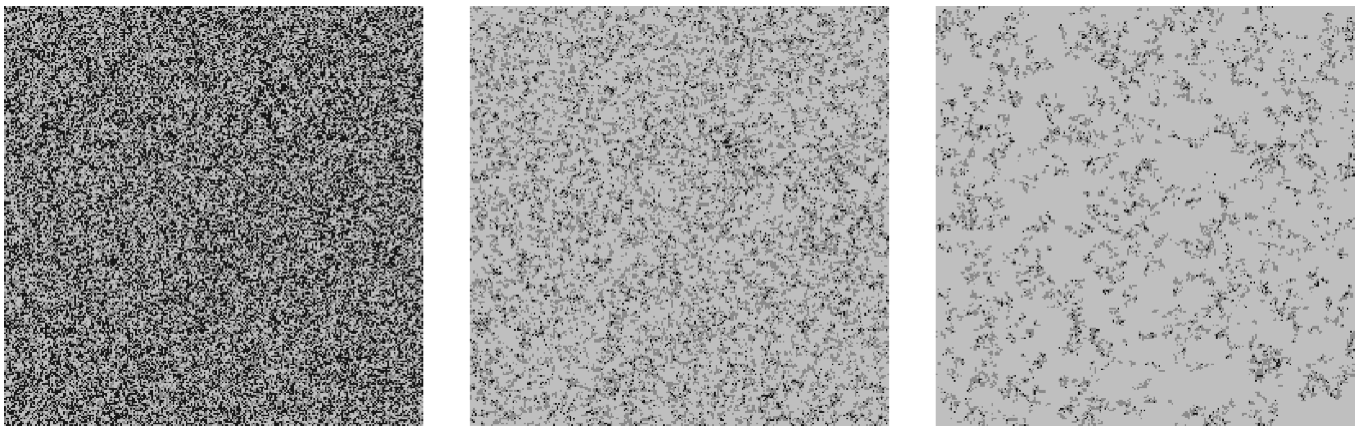

FIG. 3: Snapshots of the time evolution (time increases from left to right) of the two-dimensional SLLVM model in the species coexistence phase, but near the predator extinction threshold, when the fixed point is a node. The light, gray, and dark dots respectively represent the prey, predators, and empty sites on the lattice. The same rates, initial condition and system size apply as for Fig. 2, except that now $\lambda = 0.15$.

predators are more efficient in 'chasing' the prey). As shown in Fig. 4 (left), there is an effective repulsion at short distances (anticorrelations for small x) and an effective attraction (positive correlations $C_{A,B}(x) > 0$) at larger (but finite) distances between predators and prey. This effective 'attraction' results in the 'bumps' (rounded peaks) of Fig. 4 for a relative distance of $x = 5 - 10$ lattice sites. These facts translate pictorially in the complex patterns displayed in Fig. 2, where the prey spots are typically at a finite distance from the predators: they are 'eaten' if they come too close.

Figures 5 and 6 show that (anti-)correlations [$C_{A,A}(x) > 0$, $C_{B,B}(x) > 0$, and $C_{A,\oslash}(x) < 0$, $C_{B,\oslash}(x) < 0$ at finite distance x] develop, respectively among predators, among prey, and between predators or prey and empty sites, when λ is raised: predators (prey) effectively 'attract' each other while the predators/prey and vacancies 'repel' each other. In fact, in Fig. 2 we notice 'clusters' of predators well separated from those of empty sites. Figure 4 (right) illustrates that correlations $C_{\oslash,\oslash}(x)$ among empty sites increases with the value of λ, which results from the 'clustering' among predators and prey occurring in the coexistence phase, as shown on the rightmost of Fig. 2 (see also [38]).

Figure 7 displays, for a single realization, i.e., without sample averaging), the typical temporal behavior of the predator density $a(t)$ when the fixed point is a focus. After some initial time interval of damped oscillations (see Fig. 8), as consequence of the spatial fluctuations, the predator density oscillates in a rather erratic fashion around the average value. It is clear from the graphs that the amplitude of the oscillations in the steady state decreases with the system size; in the thermodynamic limit the amplitude of the oscillations vanishes (see Fig. 8). This remarkable feature was also reported in other stochastic lattice predator–prey systems
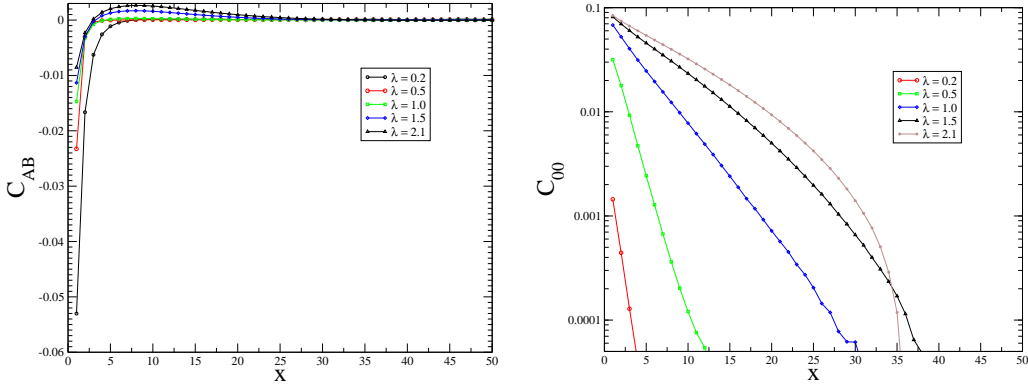
FIG. 4: (Color online.) Two-dimensional static correlation functions $C_{A,B}(x)$ (left) and $C_{\oslash,\oslash}(x)$ (right, in linear-logarithmic scale) for $\sigma = 4.0$, $D = 0$, $\mu = 0.1$, and $\lambda = 0.2, 0.5, 1.0, 1.5, 2.1$. The system size is 256×256.
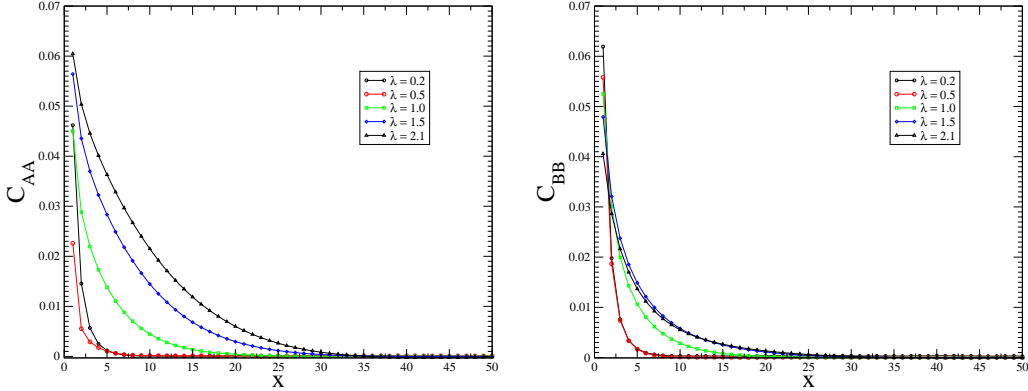

FIG. 5: (Color online.) Two-dimensional static correlation functions $C_{A,A}(x)$ (left) and $C_{B,B}(x)$ (right) for $\sigma = 4.0$, $D = 0$, $\mu = 0.1$ and $\lambda = 0.2, 0.5, 1.0, 1.5, 2.1$. The system size is 256×256.

[17, 18, 21].

For our SLLVM variant, Fig. 8 depicts the transient regime (again, for a single realization) from a random starting configuration, initially filled with $1/3$ of each of the species, toward its steady state. The plots of the densities for both species exhibit damped oscillations with a period and amplitude that is completely independent of the initial conditions, in contrast with the predictions from the standard deterministic Lotka–Volterra rate equations (2), (3). The inset in Fig. 8 shows that the Fourier component $|a(\omega)| = |\sum_t e^{i\omega t} a(t)|$ vs. $2\pi/\omega$ displays a distinct peak at around 135×5 MCS (data are taken every 5 MCS) for this set of values of the stochastic parameters, namely $D = 0$, $\lambda = 1$, $\sigma = 4$, and $\mu = 0.1$.

It is important to emphasize the fact that the amplitude of the oscillations decreases with increasing the lattice size only 'globally', i.e., if one measures the total density of the species. In contrast, if one observes the temporal evolution of the density on a small, fixed subset of the lattice then the amplitude of the oscillations on this sub-lattice remains approximately the same with increasing the volume of the system [21]. The erratic oscillations displayed in (finite) predator–prey systems have found considerable interest in the recent years. For instance, McKane and Newman [19] have considered a

zero-dimensional stochastic predator–prey model (represented as an 'urn'), and have shown that the frequency predicted by the mean-field rate equations naturally appears to be the characteristic frequency of the damped oscillations of their model and results of a stochastic resonance amplification. We have also studied the functional dependence of the characteristic frequency ω_{MC} of the damped erratic oscillations on the branching rate σ (for fixed values of λ, D and μ) for a fairly large two-dimensional lattice (but still displaying some clear erratic behavior, see Fig. 7), and compared the results with the predicted ω_{MF} arising from the mean-field theory, obtained (with $\rho = \zeta = 1$) from the imaginary part of Eq.(11): $\omega_{\mathrm{MF}} = |\Im\epsilon_{\pm}(a_3^*, b_3^*)| = \frac{\mu\sigma}{2\lambda}\sqrt{1 - \frac{4\lambda}{\sigma}\left(1 - \frac{\lambda}{\mu}\right)}$.

The results are shown in Fig. 9. We see that the characteristic frequency ω_{MC} of the SLLVM is always markedly *smaller* than the mean-field prediction ω_{MF} (by a factor $2.5\ldots3$), but the functional dependence on the parameter σ appears to be in fairly good agreement with the mean-field predictions. Yet we note that for another stochastic predator–prey model variant, Antal and Droz reported completely different functional dependence for the mean-field and Monte Carlo results [18].
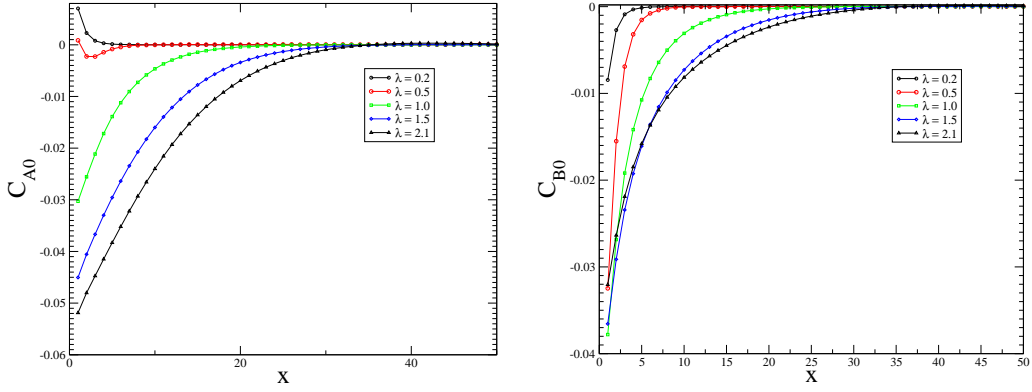
A completely different picture from that of Fig. 2

FIG. 6: (Color online.) Two-dimensional static correlation functions $C_{A,\oslash}(x)$ (left) and $C_{B,\oslash}(x)$ (right) for $\sigma = 4.0$, $D = 0$, $\mu = 0.1$ and $\lambda = 0.2, 0.5, 1.0, 1.5, 2.1$. The system size is 256×256.
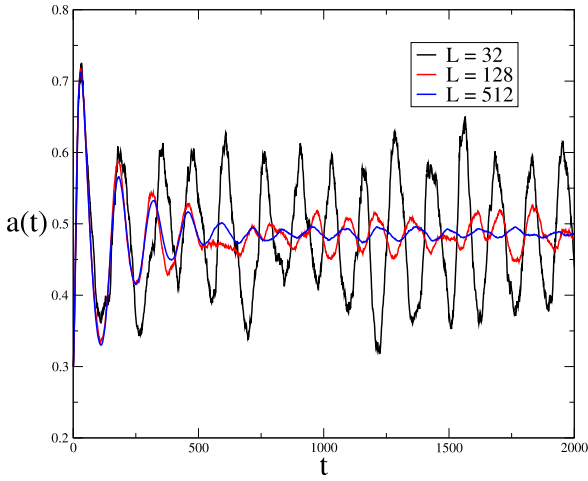

FIG. 7: (Color online.) The density of the predators $a(t)$ vs. t on two-dimensional lattices (measured for single realizations) with $L = 32$, 128 and 512. The values of the stochastic parameters are $D = 0$, $\lambda = 1$, $\sigma = 4$, and $\mu = 0.1$. Initially the particles are homogeneously distributed with densities $a(0) = b(0) = 0.3$.
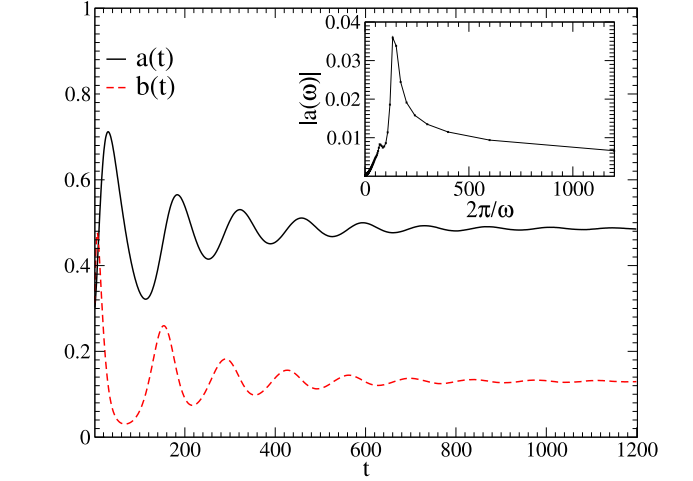
FIG. 8: (Color online.) The predator and prey densities $a(t)$ and $b(t)$ vs. t, from single runs, on a 4096×4096 lattice for $D = 0$, $\lambda = 1$, $\sigma = 4$, and $\mu = 0.1$. The inset shows the Fourier transform of the density of predators with a pronounced peak at around 135×5 MCS.

emerges when the fixed point is a node. The three plots in Fig. 3 again depict snapshots (starting with random initial configuration on the left) of the coexistence phase on a two-dimensional lattice [38]. In this case no real pattern formation takes place in the steady state; rather we notice a small number of 'clouds' (clusters) of predators effectively diffusing in a sea of prey (the rightmost picture on Fig. 3). Upon lowering the value of λ further, the average size of the predator 'clouds' and their density decreases, and the system eventually enters the absorbing phase for sufficiently small values of λ. One observes here that the dynamics of the small activity clusters close to the absorbing transition is very simple: (i) an 'active spot' can die; (ii) upon encounter two (or more) 'activities' usually coalesce; (iii) an 'active spot' can split into two (branching). Thus, as the system displays a continuous phase transition from a fluctuating active phase

into a unique stable absorbing state; as only short-range interactions are involved; and since the model is not subject to any special symmetries or conservation laws, the conditions of the so-called DP conjecture [39] are fulfilled. Therefore, the phase transition occurring in this model from an active to the absorbing phase (from the predators' viewpoint) is a good candidate for the directed percolation (DP) universality class [29, 40].

For studying the critical properties of the model for the transition from an active to an absorbing state, we employ as an order parameter the average predator density a. In the active phase, $a(t \to \infty) = a^*$ assumes a nonzero value, while in the absorbing state the lattice is full of prey and $a^* = 0$. Thus, at the critical point, the exponent β is defined according to $a^* \sim (\lambda - \lambda_c)^\beta$ [29]. The stochastic fluctuations are responsible for a shift of the critical point and changes in the critical exponents: for instance (in dimensions $1 < d \leq 4$), the actual com-

puted value of β is always smaller than the value $\beta_{\mathrm{MF}} = 1$ predicted by the mean-field analysis.

In order to check the critical properties of the two-dimensional model close to the extinction phase transition point, we employ the dynamical Monte Carlo approach with an initial configuration that has only a single active site (a predator) in the middle of the lattice, with the remainder filled with prey [29]. As an illustration, in Fig. 10 we report the dynamical Monte Carlo analysis for a 512×512 lattice with $D = 0$, $\sigma = 4.0$, and $\mu = 0.1$. In this case, the duration of the simulations was 10^5 MCS. We chose to measure the survival probability $P(t)$ [the probability that after time t we still have predators in the system], and the number of active sites (i.e. predators) $N(t)$. In order to obtain reasonably good estimates for these two quantities, we performed 3×10^6 independent runs. Close to the critical point, $P(t)$ and $N(t)$ follow algebraic power laws with critical exponents δ and θ, respectively:

$$P(t) \sim t^{-\delta'} , \qquad N(t) \sim t^{\theta} . \tag{17}$$

Figure 10 shows the effective exponents $\delta'(t)$ and $\theta(t)$ defined via

$$-\delta'(t) = \frac{\ln[P(t)/P(t/3)]}{\ln 3} ,$$
$$\theta(t) = \frac{\ln[N(t)/N(t/3)]}{\ln 3} . \tag{18}$$

Just below (above) λ_c the effective exponent graphs are supposed to curve down (up) for large t while for $\lambda = \lambda_c$ they should be more or less straight lines; their intercept gives the numerical value of the exponent. From the graphs we estimate the critical value of $\lambda_c = 0.1688(1)$ instead of the mean-field result $\lambda_c = \mu = 0.1$; as to be expected, fluctuations shift the critical point to larger values of the predation rate (suppress the 'ordered' phase).
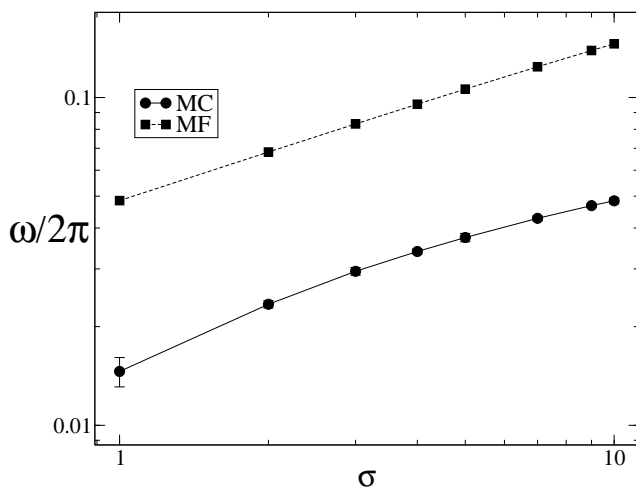

FIG. 9: Functional dependence of the characteristic frequency: comparison of mean-field prediction ω_{MF} (squares) and Monte Carlo simulations (circles) on a 128×128 lattice. The reactions rates are $\lambda = 1.6$, $\mu = 0.1$, $D = 0$.

The values for δ' and θ are very close to 0.451 and 0.230, respectively, which are the known exponents for the two-dimensional DP model [29]. For the system depicted in Fig. 10, the numerical value of the critical exponent β is also very close to the established $\beta \approx 0.584$ exponent for the two-dimensional DP model. We have checked that for other choices of the rates D, μ, and σ we also obtain critical exponents that are consistent with the DP universality class.

The Monte Carlo simulations for the three-dimensional model result in values for the critical exponents that are again very close to the established DP critical values. For instance, near the critical point, we have measured an exponent $\beta \approx 0.81$, in excellent agreement with the corresponding value, $\beta_{\mathrm{DP}} \approx 0.81(1)$ reported for DP in $d = 3$ [29]. In three dimensions, we also observe the same two different scenarios, namely isolated predator clusters near the threshold and expanding and merging activity fronts at larger predation rates, as in two dimensions, see Figs. 2 and 3). Not surprisingly, we have found that the complex patterns associated with the active focus fixed point are less correlated in $d = 3$ compared with $d = 2$. Also, for dimensions $d > 4$ we recover the mean-field critical exponents, consistent with the fact that the upper critical dimension is $d_c = 4$ for the DP universality class.

Numerical results suggesting that lattice predator-prey models exhibit an active-absorbing phase transition belonging to the DP universality class have also been reported recently for other two-dimensional model systems [17, 18, 26]. In Sec. III.D, we provide field-theoretic arguments that support the assertion that the critical properties near the predator extinction threshold in these models is indeed generically described by the DP scaling exponents (see also Ref. [30]). We have also performed Monte Carlo simulations for systems where the predation reactions were subject to a spatial bias, i.e., possible only along a special direction in two dimensions. While such a bias clearly renders the activity fronts in the active phase anisotropic, it does not seem to affect the properties near the extinction threshold. For aside from an overall slow drift along the preferred spatial direction, which sets up a net particle current, the predators still form isolated islands in a sea of prey. Hence we expect that one should observe the DP critical exponents even in this 'driven' system, see Sec. III.D below. Similarly, when the predators are made to actually 'follow' the prey, by biasing the hopping probabilities for the A species towards neighboring sites occupied by B particles, no qualitative changes from the simple SLLVM are observed. Notice that this variant of the SLLVM differs from that considered in Refs. [26]: whereas there both predators and prey were allowed to perform 'smart moves', we have allowed only the predators to 'chase' the prey by moving toward the regions where the concentration of prey is locally highest. These differences might be important as they could perhaps explain that we always observed damped erratic oscillations, whilst the authors of Refs. [26] reported the
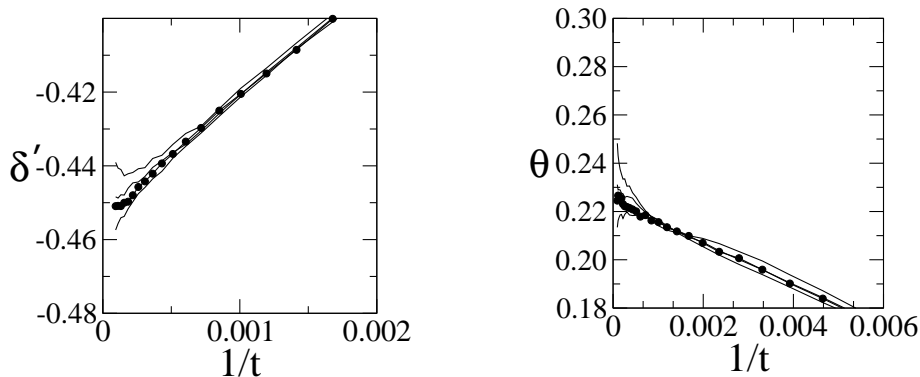
FIG. 10: Dynamical Monte Carlo simulations to estimate the predator extinction threshold λ_c for the two-dimensional (on a 512×512 lattice) NN model with $D = 0$, $\sigma = 4.0$, and $\mu = 0.1$. The effective scaling exponents $\delta'(t)$ vs. $1/t$ (on the left) and $\theta(t)$ vs. $1/t$ (on the right) are shown for four values of λ: 0.1690, 0.1689, 0.1688, and 0.1687 (from top to bottom).
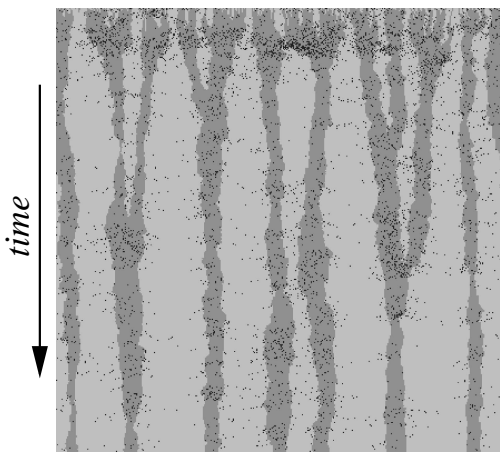

FIG. 11: Space-time plot for the one-dimensional SLLVM (with mutual predator–prey site restrictions), starting from a random initial configuration with homogeneous density distribution, $a(0) = 0.5 = b(0)$ (top row; time proceeds downwards). Multi-strip metastable configurations are observed for a long time while the system slowly evolves toward the absorbing steady state devoid of predators. The system size here is $L = 1024$, and for the parameters we chose $D = 1$, $\mu = 0.0005$, $\sigma = 0.01$, and $\lambda = 0.008$. The light gray, dark gray, and black dots respectively represent the prey, predators, and empty sites.

existence (in $d = 2$) of self-sustained oscillations.

To conclude this section, we briefly consider the one-dimensional case. It is well-known that site restrictions may become quite crucial in one spatial dimension [36, 41, 42], one must be prepared to encounter special behavior in this case. Indeed, since in our version of the SLLVM we are not allowing simultaneous site occupation by the predators and prey, in contrast with Refs. [17, 18], the A and B populations may be forced to segregate into distinct domains on a one-dimensional lattice (see the similar mechanisms for other multi-species reaction–diffusion systems reported in Refs. [41, 42]). The results of our computer simulations in fact show that the steady

state of the one-dimensional system is a lattice full of prey for *all* values of the stochastic parameters. If we start from a random initial configuration we observe that the system 'coarsens' (as in the one-dimensional three-species cyclic Lotka–Volterra model, see Ref. [23] and the end of Sec. I): it slowly evolves into configurations of repeating sequences of domains of predators and prey. The spatio-temporal plot of a typical run is shown in Fig. 11. This multi-domain configuration constitutes a long-lived metastable state in the one-dimensional system, and typically an enormous crossover time must elapse for the system to reach the steady state, even in our finite lattices. As time increases, domains ('stripes') of predators merge in a sea of prey (with some sparse holes) and eventually, in the steady state, the number of these stripes of predators vanishes for any set of values of the stochastic parameters; the final system is full of prey.

We have indeed found the width of a single predator–hole domain to remain constant upon increasing the system size, which is typical of a coarsening phenomenon, and supports the previous observation that asymptotically, in the thermodynamic limit, one arrives at a steady state with vanishing predator density. We might think of the effective long-time coarse-grained dynamics of the predator and prey domains as being described by the simple coagulation/decay reactions $\tilde{A} + \tilde{A} \to \tilde{A}$ and $\tilde{A} \to \emptyset$. where $\tilde{A}$ represents a predator–hole domain, and $\emptyset$ indicates a prey domain. As $t \to \infty$, this would suggest that the predator density should decay as a power law $\sim t^{-1/2}$, ultimately turning over to an exponential cutoff. Owing to the huge crossover times in this system, we were not able to confirm this conjecture quantitatively. Yet the same kind of behavior was reported in Ref. [21] for the one-dimensional version of the cyclic three-state SLLVM. Notice, however, that since in the four-state models of Refs. [17, 18] predator and prey particles were allowed to occupy the same lattice sites, species segregation did not occur in the simulations reported there.

D. Field-theoretic analysis of the continuous predator extinction transition

We have seen that our Monte Carlo simulations in two and three dimensions in many ways confirm the *qualitative* picture from the mean-field predictions, once growth-limiting terms are taken into account there. However, the mean-field approximation naturally cannot capture the intriguing dynamical spatial structures in the active coexistence phase of the SLLVM. Moreover, it does not aptly describe the universal scaling properties near the predator extinction threshold. In the language of nonequilibrium statistical mechanics, and with respect to the predator population, this constitutes a continuous phase transition from an active phase to an inactive, absorbing state. For local interactions, and in the absence of additional conservation laws and quenched disorder, such active to absorbing state phase transitions are known to be generically described by the universality class of directed percolation (DP) [39] (for recent reviews, see Refs. [29]). Since this is true even for many-species systems [30], one would expect the extinction threshold in the SLLVM to be governed by the DP exponents as well, as was indeed suggested in Refs. [16, 17, 18]. In the preceding Sec. III.C, we have added further evidence from our Monte Carlo simulation data that the critical exponents in the SLLVM are consistent with those of DP.

We now proceed to provide field-theoretic arguments, based on a standard mapping of the master equation corresponding to the SLLVM processes, i.e., the spatial extension of Eq. (5). For the sake of clarity, before providing our field-theoretic analysis of the SLLVM, we briefly outline the general approach (see Ref. [40] and references therein). The first step towards a field-theoretic treatment is to recast the master equation (13) into the stochastic (quasi-)Hamiltonian formulation [36], the site restrictions being implemented into a second quantization bosonic formalism (to avoid a more cumbersome representation in terms of spin operators) [43]. One then proceeds by adopting a coherent-state path integral representation and by taking the continuum limit. This leads to an Euclidean action S which embodies the statistical weight of each possible configuration and is the central ingredient to perform perturbative renormalization group (RG) calculations (the bilinear part of the action being identified as the Gaussian reference action). Here, our goal is to show that the action of the SLLVM can be mapped onto a field theory known to share the same critical properties as the DP. In addition, the field-theoretic treatment allows us to systematically discriminate between processes which are relevant/irrelevant for the critical properties of the SLLVM (in the RG sense) and thus identify robust features of the stochastic lattice predator-prey systems.

At this point, we specifically turn to field-theoretic analysis of the SLLVM. The essence of the following treatment is simply the observation that the prey population is nearly homogeneous and constant near the predator extinction threshold. The processes involving the prey then effectively decouple, and the SLLVM reactions essentially reduce to $A \to \oslash$ and $A \to A + A$. Yet this set of processes, supplemented with either the growth-limiting reaction $A + A \to A$ or site restrictions for the A particles, is just prototypical for DP [29]. Following the aforementioned standard procedures [40], the field theory action for the combined processes $A \to \oslash$ (rate μ), $B \to B + B$ (rate σ), and $A + B \to A + A$ (rate λ), along with particle diffusion, becomes (omitting temporal boundary terms):

$$
\begin{aligned}
S[\hat{a}, a; \hat{b}, b] \;=\; & \int d^d x \int dt \Big[\hat{a} \left(\partial_t - D_A \nabla^2 \right) a \qquad (19) \\
& + \hat{b} \left(\partial_t - D_B \nabla^2 \right) b + \mu \left(\hat{a} - 1 \right) a \\
& + \sigma \left(1 - \hat{b} \right) \hat{b}\, b\, e^{-\rho^{-1} \hat{b} b} + \lambda \left(\hat{b} - \hat{a} \right) \hat{a}\, a\, b \Big] .
\end{aligned}
$$

Since we are interested in the critical properties near the extinction threshold, where there remains almost no predators in the system, we do not need to take into account any spatial restriction imposed on the prey species by the A particles, and therefore have set $\zeta \to \infty$ in Eq. (19). Note that D_A and D_B here are the *effective* diffusivities for the two species that in the site-restricted system emerge as a consequence of the offspring production on neighboring sites (even if there is no hopping present in the microscopic model). The fields $\hat{a}$ ($\hat{b}$) and a (b) originate from the coherent-state left and right eigenvalues of the bosonic creation and annihilation operators in the stochastic (quasi-)Hamiltonian for the predators (prey). The Trotter formula combined with the discrete hopping processes yields the diffusion propagators in the action (19), while the reactions are encoded in the terms proportional to the rates μ, σ, and λ. In each of these terms, the first contribution indicates the 'order' of the reaction (namely, which power of the particle densities $\hat{a}\, a$ and $\hat{b}\, b$ enters the rate equations), whereas the second contribution directly encodes the process under consideration (a and b annihilate a predator or prey particle, $\hat{a}$ and $\hat{b}$ create them).

The exponential in the prey reproduction term captures the site restrictions within the bosonic field theory [43]; the parameter ρ, with dimension of a particle density, emerges upon taking the continuum limit. In terms of an arbitrary momentum scale κ, the scaling dimension of ρ^{-1} is therefore κ^{-d}, and it constitutes an irrelevant coupling in the renormalization group sense. However, since it is essential for the existence of the phase transition, we may not set $\rho^{-1} = 0$ outright, despite the fact that it does scale to zero under repeated scale transformations. Rather, we may expand $e^{-\rho^{-1} \hat{b} b} \approx 1 - \rho^{-1} \hat{b} b$, but need to retain the first-order contribution. The classical field equations $\delta S / \delta a = 0 = \delta S / \delta b$ are solved by $\hat{a} = 1 = \hat{b}$ (as a consequence of probability conservation [40]), whence $\delta S / \delta \hat{a} = 0 = \delta S / \delta \hat{b}$ then essentially yield the mean-field equations of motion (12) for $\zeta^{-1} = 0$,

and we may identify ρ^{-1} with the prey carrying capacity. Upon shifting the fields $\hat{a} = 1 + \tilde{a}$, $\hat{b} = 1 + \tilde{b}$, the action then reads

$$
\begin{aligned}
S[\tilde{a}, a; \tilde{b}, b] = \int d^d x \int dt \Big[&\tilde{a} \left(\partial_t - D_A \nabla^2 + \mu \right) a \\
&+ \tilde{b} \left(\partial_t - D_B \nabla^2 - \sigma \right) b - \sigma \, \tilde{b}^2 \, b \\
&+ \sigma \, \rho^{-1} \, (1 + \tilde{b})^2 \, \tilde{b} \, b^2 - \lambda \, (1 + \tilde{a}) \, (\tilde{a} - \tilde{b}) \, a \, b \Big] . \quad (20)
\end{aligned}
$$

For vanishing predation rate $\lambda = 0$, the A and B processes of course decouple, with the predators dying out (with rate μ), whereas the prey population is at its carrying capacity, $b \approx \rho$. We are interested in the properties near the predator extinction threshold at λ_c (in mean-field theory, $\lambda_c = \mu/\rho$), where also $a \to 0$ and $b \to b_s \approx \rho$. We therefore introduce the fluctuating field $c = b_s - b$, and demand that $\langle c \rangle = 0$, which eliminates the linear source term $\sim b_s \tilde{c}$ in the ensuing action. With $\tilde{c} = -\tilde{b}$, we obtain

$$
\begin{aligned}
S[\tilde{a}, a; \tilde{c}, c] = \int d^d x \int dt \, \Big[&\tilde{a} \left(\partial_t - D_A \nabla^2 + \mu - \lambda \, b_s \right) a \\
&+ \tilde{c} \left[\partial_t - D_B \nabla^2 + (2b_s/\rho - 1) \, \sigma \right] c + \sigma \, b_s (2b_s/\rho - 1) \, \tilde{c}^2 \\
&- \sigma \, \rho^{-1} \, b_s^2 \, \tilde{c}^3 - \sigma \, (4b_s/\rho - 1) \, \tilde{c}^2 \, c - \sigma \, \rho^{-1} \, (1 + \tilde{c}^2) \, \tilde{c} \, c^2 \\
&+ 2\sigma \, \rho^{-1} \, \tilde{c}^2 \, (c + b_s \, \tilde{c}) \, c - \lambda \, b_s \left[\tilde{a}^2 + (1 + \tilde{a}) \, \tilde{c} \right] a \\
&+ \lambda \, (1 + \tilde{a}) \, (\tilde{a} + \tilde{c}) \, a \, c \Big] . \quad (21)
\end{aligned}
$$

We now exploit the fact that the prey density is hardly fluctuating, as encoded in the mass term $\approx \sigma$ for the $\tilde{c} \, c$ propagator. Thus upon rescaling $\phi = \sqrt{\sigma} \, c$ and $\tilde{\phi} = \sqrt{\sigma} \, \tilde{c}$, and letting $\sigma \to \infty$ (the scaling dimension of the branching rate σ is κ^2, whence it constitutes a relevant variable that will flow to infinity under the RG), the nonlinear terms in the prey fields disappear, and the predator and prey sectors effectively decouple,

$$
\begin{aligned}
S_\infty[\tilde{a}, a; \tilde{\phi}, \phi] \;=\; \int d^d x \int dt \, \big[&\tilde{a} \left(\partial_t - D_A \nabla^2 + \mu - \lambda \, b_s \right) a \\
&- \lambda \, b_s \, \tilde{a}^2 \, a + \tilde{\phi} \, \phi + b_s \, \tilde{\phi}^2 \big] . \quad (22)
\end{aligned}
$$

The fields ϕ and $\tilde{\phi}$ are now readily integrated out; for the predators, however, we need to implement a growth-limiting term as originally enforced through the finite supply of prey. This is done most easily through adding the reaction $A + A \to A$ with rate τ. In the field theory action, this leads to the additional terms $\tau \, (\hat{a} - 1) \, \hat{a} \, a^2 = \tau \, \tilde{a} \, (1 + \tilde{a}) \, a^2$. Setting $D_A \, r_A = \mu - \lambda \, b_s$, and rescaling the fields to $\mathcal{S} = \sqrt{\lambda \, b_s / \tau} \, a$ and $\tilde{\mathcal{S}} = \sqrt{\tau / \lambda \, b_s} \, \tilde{a}$, we finally arrive at

$$
\begin{aligned}
S_\infty[\tilde{\mathcal{S}}, \mathcal{S}] \;=\; \int d^d x \int dt \, \Big[&\tilde{\mathcal{S}} \Big(\partial_t + D_A \left(r_A - \nabla^2 \right) \Big) \mathcal{S} \\
&- u \, \tilde{\mathcal{S}} \left(\tilde{\mathcal{S}} - \mathcal{S} \right) \mathcal{S} + \tau \, \tilde{\mathcal{S}}^2 \, \mathcal{S}^2 \Big] , \quad (23)
\end{aligned}
$$

where $u = \sqrt{\tau \, \lambda \, b_s}$. Since the scaling dimensions of both λ and τ are κ^{2-d}, and b_s represents a particle density, the scaling dimension of the new effective nonlinear coupling u^2 is κ^{d-4}. Thus the upper critical dimension of the effective field theory (23) for the predator extinction threshold is $d_c = 4$, and the four-point vertex $\propto \tau$ is irrelevant in the RG sense near d_c. If we are interested only in asymptotic universal properties, we may thus drop this vertex, which leaves us precisely with Reggeon field theory that describes the critical properties of DP clusters [28, 29]. Notice, however, that the above treatment does not apply to one dimension, if we consider hard-core particles or site exclusion; as observed in other reaction–diffusion models as well [41, 42], the one-dimensional topology then induces species segregation, and in the system under consideration here, the active coexistence state disappears entirely.

We remark that the above processes also generate $A + B \to A$, $A + B \to \oslash$, $B \to B + B + B$ etc. on a coarse-grained level. These reactions can be readily included in the previous analysis, without any qualitative changes in the final outcome: the continuous active to absorbing state phase transition for the predator population A is in any case described by the DP critical exponents. We had previously mentioned another variant, where the predation process is spatially biased along a given direction. If we mimic such a situation by an additional vertex of the form $-E \nabla_\parallel S^2$ (where the spatial derivative $\nabla_\parallel$ is along the drive direction), which is characteristic of driven diffusive systems [37], we note that since its scaling dimension is $[E] = \kappa^{2-d}$, it should be irrelevant at the extinction threshold, and the critical exponents of the phase transition still be described by DP. (This argument assumes, however, that the drive nonlinearity does *not* induce an anisotropy in the spatial ordering; if only the spatial sector transverse to the drive softens, while the longitudinal fluctuations remain noncritical, novel critical behavior may ensue.)

IV. CONCLUSION

We have studied the effect of spatial constraints and stochastic noise on the properties of the Lotka–Volterra model, which is a generic two-species predator–prey system defined on a lattice interacting via a predation reaction that involves nearest neighbors. We obtain a rich collection of results that differ remarkably from the predictions of the classical (unrestricted) deterministic Lotka–Volterra model. This investigation was carried out both analytically, using a suitable mean-field approach and field-theoretic arguments, as well numerically, employing Monte Carlo simulations. (In this paper, we have mainly presented figures obtained from two-dimensional simulations, the most ecologically relevant situation, but we have also checked our statements running simulations in one, three, and four dimensions.)

The mean-field analysis of the stochastic lattice Lotka-Volterra model (SLLVM) [7] predicts that there is a continuous non-equilibrium phase transition from an active

(species coexistence) to an absorbing (full of prey) state and these predictions are confirmed, in dimensions $d > 1$, by the computer simulations. Already in other stochastic lattice predator–prey models, it was shown that the mean-field description provided this type of behavior (see, e.g., Refs. [16, 18, 26]). From an ecological and biological perspective, this means that the rate equations, when they take into account limited local resources, predict a possible extinction of one population species (here, the predators), which is a realistic feature absent from the conventional Lotka–Volterra rate equations [7].

Actually, in contrast to the cyclic three-state SLLVM of Ref. [21] and other stochastic predator-prey models [17], here the mean-field predictions capture the essential qualitative features of the SLLVM phase diagram in dimensions $d > 1$. Our field-theoretic analysis shows that the mean-field critical exponents are quantitatively valid in dimensions $d > d_c = 4$. According to the mean-field analysis and the Monte Carlo simulations, the stable coexistence fixed points of this model can be either nodes or foci. It does not exhibit stable and persistent population oscillations but only damped and transient ones, near a stable focus, whose amplitudes vanish in the thermodynamic limit. However, these erratic oscillations are quite persistent in finite systems and should dominate the dynamics of even fairly large, but finite populations for many generations, see Figs. 7 and 8. These features, which appear to be more realistic from an ecological point of view than the regular (and initial-conditions dependent) oscillations predicted by the conventional Lotka–Volterra equations, have been observed in other stochastic lattice predator–prey models as well [16, 17, 18, 21, 31], and likely represent a generic feature of such systems. This possibly has direct implications as it might shed further light on issues of particular ecological and biological relevance, such as the emergence of (quasi-)oscillatory behavior and spontaneous pattern formation as results of stochastic fluctuations.

Typically, in two and three dimensions, when the fixed point is a focus (at large values of the predation rate λ), the species coexistence phase is characterized by the formation of complex and correlated patterns, as the result of the interaction and the propagation of the traveling wave fronts of predators and prey, which in turn cause the overall population oscillations [38]. The spatial structure of these patterns have been studied by computing the correlations functions, whilst their dynamical properties have been investigated through the computation of the functional dependence of the frequency of the resulting oscillations. We have found that the typical frequency of the stochastic oscillations are markedly reduced by fluctuation effects (i.e., compared to the mean-field predictions).

Near their extinction threshold in the coexistence regime, the predators are largely localized in clusters interspersed in a sea of prey, with an active reaction zone at their boundaries [38]. We have carefully analyzed the critical properties of the system by computing various critical exponents and have checked that the active to absorbing phase transition belongs to the directed percolation (DP) universality class, with upper critical dimension $d_c = 4$. Field-theoretic arguments support this conclusion: starting from the master equation, we have constructed a field theory representation of the involved stochastic processes, which near the predator extinction threshold can be mapped onto Reggeon field theory. By utilizing tools of statistical mechanics (mean-field treatment together with field-theoretic and renormalization group arguments) we thus obtain a general qualitative understanding of the properties of the system and also a quantitative predictions of its behavior in the vicinity of the extinction threshold. In particular, the critical exponents governing the various statistical properties of the populations densities near the threshold are argued to be the same as in directed percolation (in dimensions $d > 1$). Also, active to absorbing state phase transitions and DP critical exponents were (numerically) reported in studies of other stochastic lattice predator–prey model variants [17, 18, 25, 26, 31]. Thus, our field-theoretic analysis should apply to a broader class of stochastic models than the ones considered here.

We have also discussed the one-dimensional case where, due to its special topology, the site occupation restriction on the lattice imply a 'caging effect' resulting in species segregation and very slow coarsening of the predator domains in the system, which eventually evolves towards a lattice filled with prey.

Finally, we remark that in stark contrast with the deterministic Lotka–Volterra system, whose mathematical features are well-known to be quite unstable with respect to any model perturbations, the *stochastic* spatial version is quite generic, and its overall features are rather robust against model variations. In particular, as noted also in Refs. [17, 21], we have checked that the presence or absence of explicit particle diffusion does not qualitatively affect the properties of the system, since in our site-restricted system species proliferation is generated by the offspring production processes. Similarly, we have found that when the predation process is spatially biased, near the extinction threshold only non-universal details change, but the DP critical behavior still applies, and more generally, the overall picture drawn here remains valid in the active coexistence phase as well. An intriguing situation is obtained when one considers a stochastic lattice predator-prey system with a next-nearest-neighbor (NNN) interaction among the competing species, as well as a short-range exchange process [31]. In this case a subtle interplay emerges between the NNN interaction and the nearest-neighbor (NN) exchange or 'mixing': When the latter is 'slow', due to the presence of correlations, this system also undergoes a DP-type phase transition (in dimensions $1 < d \leq 4$), as does the SLLVM studied in this work [31]. However, when the value of the mixing rate is raised, the simple short-range exchange processes 'wash out' the correlations and the system undergoes a *first-order phase transition* as in fact predicted

by mean-field theory [31]. Whereas the rate equations predict entirely different behavior of the NNN system, which once more reflects the instability of the classical Lotka–Volterra model, it is quite remarkable that in the absence of explicit species mixing through particle exchange, the fluctuations render the properties of the NNN model akin to the simple SLLVM with only nearest-neighbor interactions. In marked contrast with its mean-field counterpart, the stochastic lattice Lotka–Volterra model is thus quite stable with respect to model modifications. On the other hand, as the mean-field regime is expected to be reached when the exchange process allows the mixing of *all* the particles (and not only the immediate nearest neighboring ones) with an infinitely fast rate [13], the fact that mean-field like behavior, characterized by a first-order phase transition, already appears unexpectedly even for finite NN exchange rates [31] is another quite intriguing feature of the NNN model. This is even more surprising since we have checked that fast diffusion affects neither the critical nor the qualitative properties of the SLLVM studied in this paper.

Acknowledgments

APPENDIX A: KOLMOGOROV'S THEOREM AND BENDIXSON–DULAC TEST

In this appendix, we discuss the application of a general theorem due to Kolmogorov [8] and of the so-called Bendixson–Dulac [11] to the coupled rate equations (6) and (7).

We start with a theorem by Kolmogorov, who studied the mathematical properties of two-species (mean-field type) rate equations of predator–prey models of the following form [3, 8]:

$$\dot{a}(t) = a(t)\,G(a(t), b(t)) , \qquad (A1)$$
$$\dot{b}(t) = b(t)\,F(a(t), b(t)) , \qquad (A2)$$

Kolmogorov demonstrated that the generic system (A1), (A2) is characterized *either* by a stable fixed point *or* by a limit cycle, if F and G satisfy the following conditions [3]:

$$\frac{\partial F}{\partial a} < 0 \quad ; \quad b\,\frac{\partial F}{\partial b} + a\,\frac{\partial F}{\partial a} < 0 ; \quad (A3)$$
$$b\,\frac{\partial G}{\partial b} + a\,\frac{\partial G}{\partial a} > 0 \quad ; \quad F(0,0) > 0 ; \qquad (A4)$$
$$\frac{\partial G}{\partial a} < 0. \qquad (A5)$$

In addition, there should exist three positive quantities, $k_i > 0$ $(i = 1, 2, 3)$, such that $F(0, k_1) = 0$, $F(k_2, 0) = 0$, $G(k_3, 0) = 0$, and $k_2 > k_3$.

We now consider the models studied Sec. II.C and apply Kolmogorov's theorem to these systems. In the case considered there, we specifically have:

$$F(a, b) = \sigma\left(1 - \zeta^{-1}\,a - \rho^{-1}\,b\right) - \lambda\,a, \qquad (A6)$$
$$G(a, b) = \lambda\,b - \mu. \qquad (A7)$$

Thus, condition (A5) is not fulfilled since $\partial G/\partial a = 0$. This means that Kolmogorov's theorem does not apply here (not even in the complete absence of growth-limiting terms, i.e., for $\zeta = \rho = \infty$) and cannot ensure the existence of a stable fixed point or a limit cycle.

We now turn to the Bendixson–Dulac method which is a general approach to test whether a dynamical system of two two coupled differential equations admits periodic orbit solution. This method generally applies to any differential equation system $\dot{\boldsymbol{x}} = \boldsymbol{f}(\boldsymbol{x})$ of two variables $\boldsymbol{x} = (x_1, x_2)$, and states that there are no periodic orbits if $\mathrm{div}\,\boldsymbol{f}(\boldsymbol{x}) = \partial_{x_1}f_1(\boldsymbol{x}) + \partial_{x_2}f_2(\boldsymbol{x}) \neq 0$ and has only *one* sign in the whole space. As a consequence, for a strictly positive function $\mathcal{B}(\boldsymbol{x})$, if $\mathrm{div}\,(\mathcal{B}(\boldsymbol{x})\boldsymbol{f}(\boldsymbol{x})) \neq 0$ and does not change its sign in the whole space, then $\dot{\boldsymbol{x}} = \boldsymbol{f}(\boldsymbol{x})$ admits no periodic orbit [32]. In addition, if $\mathrm{div}\,(\mathcal{B}(\boldsymbol{x})\boldsymbol{f}(\boldsymbol{x})) = 0$, there exists a constant of motion for the original equation $\dot{\boldsymbol{x}} = \boldsymbol{f}(\boldsymbol{x})$ [11, 32].

Here, following the lines of Ref. [11] (Chap. 4), we apply the general Bendixson–Dulac method to Eqs. (6), (7) by rewriting the latter as $\dot{a} = f_1 = a\,G(a, b)$ and $\dot{b} = f_2 = b\,F(a, b)$. We then consider a Dulac (auxiliary) function $\mathcal{B} = a^{\alpha-1}b^{-1}$ and apply the Bendixson–Dulac test. By computing the divergence of $(\mathcal{B}f_1, \mathcal{B}f_2)$ and choosing $\alpha = \sigma/\rho\lambda$, one finds $\mathrm{div}\,(\mathcal{B}(\boldsymbol{x})\boldsymbol{f}(\boldsymbol{x})) = \partial_a(\mathcal{B}f_1) + \partial_b(\mathcal{B}f_2) = -\mu\alpha\mathcal{B}$. Thus, according to the Bendixson–Dulac criterion [11, 32] the existence of periodic orbits would require $\mathrm{div}\,(\mathcal{B}(\boldsymbol{x})\boldsymbol{f}(\boldsymbol{x})) = 0$. Hence, for Eqs. (6) and (7), periodic orbits are only possible when $\alpha = \sigma/\rho\lambda = 0$, i.e., for an infinite carrying capacities of prey, $\rho = \infty$.

In summary, Eqs. (6), (7) with finite (positive) rates μ, σ, and λ, do *not* admit periodic orbits, except when $\rho = \infty$. In this special case, the Bendixson–Dulac method ensures that there exists a constant of motion [11].

[1] A. J. Lotka, Proc. Natl. Acad. Sci. U.S.A. **6**, 410 (1920); A. J. Lotka, J. Amer. Chem. Soc. **42**, 1595 (1920).

[2] V. Volterra, Mem. Accad. Lincei **2**, 31 (1926); V. Volterra, *Leçons sur la théorie mathématique de la lutte pour la vie* (Gauthiers-Villars, Paris 1931).

[3] *Theoretical Ecology*, edited by R. M. May (Sinauer Associates, Sunderland, 1981); *Population Regulation and Dynamics*, Proceedings of a Royal Society discussion meeting, edited by M. P. Hassel and R. M. May (London, The Royal Society, 1990); R. M. May, *Stability and Complexity in Model Ecosystems*, (Princeton University Press, Princeton, 1973).

[4] H. Haken, *Synergetics* (Springer-Verlag, New York, 3rd ed. 1983).

[5] D. Neal, *Introduction to Population Biology* (Cambridge University Press, Cambridge, 2004).

[6] J. Maynard Smith, *Models in Ecology* (Cambridge University Press, Cambridge, 1974).

[7] J. D. Murray, *Mathematical Biology* Vols. I and II (Springer-Verlag, New York, 2002).

[8] A. N. Kolmogorov, *Sulla Teoria di Volterra della Lotta per l'Esistezza*, Giorn. Instituto Ital. Attuari, 7, 74-80 (1936).

[9] N. S. Goel, S. C. Maitra and E. W. Montroll, Rev. Mod. Phys. **43**, 231 (1971).

[10] G. Picard and T. W. Watson, Phys. Rev. Lett. **48**, 1610 (1982).

[11] J. Hofbauer and K. Sigmund, *Evolutionary Games and Population Dynamics* (Cambridge University Press, Cambridge, 1998).

[12] R. M. May and W. Leonard, SIAM J. Appl. Math. **29**, 243 (1975).

[13] R. Durrett, SIAM Review **41**, 677 (1999).

[14] C. Elton and M. Nicholson, J. Anim. Ecol. **11**, 215 (1942).

[15] P. Rohani, R. M. May, and M. P. Hassell, J. Theor. Biol. **181**, 97 (1996); *Modeling Spatiotemporal Dynamics in Ecology*, edited by J. Bascompte and R. V. Solé, (Springer, 1998).

[16] J. E. Satulovsky and T. Tomé, Phys. Rev. E **49**, 5073 (1994).

[17] A. Lipowski and D. Lipowska, Physica A **276**, 456 (2000); A. Lipowski, Phys. Rev. E **60**, 5179 (1999); M. Kowalick, A. Lipowski, and A. L. Ferreira, *ibid.* **66**, 066107 (2002).

[18] T. Antal and M. Droz, Phys. Rev. E 63, 056119 (2001).

[19] A. J. McKane and T. J. Newman, Phys. Rev. Lett. **94**, 218102 (2005).

[20] S. R. Dunbar, J. Math. Biol. **17**, 11 (1983); Trans. Amer. Math. Soc. **268**, 557 (1984).

[21] A. Provata, G. Nicolis, and F. Baras, J. Chem. Phys. **110**, 8361 (1999); G. A. Tsekouras and A. Provata, Phys. Rev. E **65**, 016204 (2001).

[22] H. Matsuda, N. Ogita, A. Sasaki, and K. Satō, Prog. Theor. Phys. **88**, 1035 (1992).

[23] L. Frachebourg and P. L. Krapivsky, J. Phys. A **31**, L287 (1998); L. Frachebourg, P. L. Krapivsky, and E. Ben-Naim, Phys. Rev. E **54**, 6186 (1996); Phys. Rev. Lett. **77**, 2125 (1996); G. Szabó and T. C. Czáran, Phys. Rev.

[24] E. Bettelheim, O. A. Nadav, and N. M. Shnerb, Physica E **9**, 600 (2001); N. M. Shnerb and O. Agam, `e-print cond-mat/9903408`.

[25] N. Boccara, O. Roblin and M. Roger, Phys. Rev. E **50**, 4531 (1994).

[26] A. F. Rozenfeld and E. V. Albano, Physica A **266**, 322 (1999); R. Monetti, A. F. Rozenfeld, and E. V. Albano, Physica A **283**, 52 (2000); A. F. Rozenfeld and E. V. Albano, Phys. Rev. E **63**, 061907 (2001); A. F. Rozenfeld and E. V. Albano, Phys. Lett. A **332**, 361 (2004).

[27] M. Droz and A. Pekalski, Phys. Rev. E **63**, 051909 (2001).

[28] W. Kinzel, in *Percolation structures and concepts*, Annals of the Israel Physical Society **5**, 425 (1983); P. Grassberger, J. Phys. A **29**, 7013 (1996).

[29] H. Hinrichsen, Adv. Phys. **49**, 815 (2000); H. K. Janssen and U. C. Täuber, Ann. Phys. (NY) **315**, 147 (2005).

[30] H. K. Janssen, J. Stat. Phys. **103**, 801 (2001).

[31] M. Mobilia, I. T. Georgiev, and U. C. Täuber, Phys. Rev. E **73**, 040903(R) (2006); `e-print:q-bio.PE/0508043`.

[32] D. W. Jordan and P. Smith, *Nonlinear Ordinary Differential Equations*, (Oxford University Press, Oxford, 3rd ed. 1999).

[33] J. Riordan, C. R. Doering, and D. ben-Avraham, Phys. Rev. Lett. **75**, 565 (1995).

[34] L. Pechenik and H. Levine, Phys. Rev. E **59**, 3893 (1999).

[35] Y. Fujii and M. Wadati, J. Phys. Soc. Jpn **66**, 3770 (1997); M. Mobilia and P.-A. Bares, Phys. Rev. E **63**, 036121 (2001).

[36] *Nonequilibrium Statistical Mechanics in One Dimension*, edited by V. Privman (Cambridge University Press, Cambridge, 1997); F. C. Alcaraz, M. Droz, M. Henkel, and V. Rittenberg, Ann. Phys. (N.Y.) **230**, 250 (1994); M. Henkel, E. Orlandini, and J. Santos, *ibid.* **259**, 163 (1997); D. C. Mattis and M. L. Glasser, Rev. Mod. Phys. **70**, 979 (1998).

[37] B. Schmittmann abd R. K. P. Zia, in: *Phase Transitions and Critical Phenomena*, Vol. 17, edited by C. Domb and J. L. Lebowitz (Academic Press, New York, 1995).

[38] Two movies ('L256.mpg' and 'L512.mpg') corresponding to the situation of Fig. 2 (but with $\lambda = 2.1$ and lattice sizes 256×256 and 512×512), as well as one movie ('movie3.mpg') corresponding to the situation of Fig. 3 (but with $\lambda = 0.18$ and lattice size 256×256) can be found at `http://www.phys.vt.edu/~tauber/PredatorPrey/movies/` .

[39] H. K. Janssen, Z. Phys. B **42**, 151 (1981); P. Grassberger, Z. Phys. B **47**, 365 (1982).

[40] U. C. Täuber, M. J. Howard, and B. P. Vollmayr-Lee, J. Phys. A: Math. Gen. **38**, R79 (2005).

[41] G. Ódor and N. Menyhárd, Physica D **168**, 305 (2002).

[42] O. Deloubrière, H. J. Hilhorst, and U. C. Täuber, Phys. Rev. Lett. **89**, 250601 (2002); H. J. Hilhorst, O. Deloubrière, M. J. Washenberger, and U. C. Täuber, J. Phys. A: Math. Gen. **37**, 7063 (2004).

[43] F. van Wijland, Phys. Rev. E **63**, 022101 (2001).